Thesis

On the potential morpho-mechanical link between the gluteus maximus and pelvic floor tissues

submitted by

Maximilian Benedikt Siess

in partial fulfillment of the requirements for the degree of

Doktor der gesamten Heilkunde

(Dr. med. univ.)

at the

Medical University of Graz

executed at the

Division of Macroscopic and Clinical Anatomy

under the supervision of

Niels Hammer, MD, Professor of Anatomy

Graz, 27th of October 2023

Declaration of Academic Integrity

Declaration of Academic Integrity I hereby confirm that the present diploma thesis is the result of my own independent scholarly work. I also confirm that in all cases, where material from the work of others (in books, articles, essays, dissertations, and on the internet) is acknowledged, quotations and paraphrases are clearly indicated. No material other than that cited in the reference list has been used. I have read and understood the Medical University's regulations and procedures concerning plagiarism.

Graz, 27th of October 2023 *Maximilian Siess m.p.*

Acknowledgements

I am extremely grateful to Univ.-Prof. Dr. med. Niels Hammer for his invaluable guidance and assistance throughout my thesis. A huge thanks also to Dr. med Johann Zwirner who provided incredibly helpful advice at all stages of the study. I would like to extend my appreciation to Priv.-Doz. Dr. rer. medic. Hanno Steinke for providing the plastinates for this study. I am also grateful to Sen. Lecturer Priv.-Doz.in Dr.in med. univ. Ulrike Pilsl for her valuable academic insights during the initial stages of this thesis. Additionally, special acknowledgments go to Manfred Eder and Gerald Waltl for their assistance with the tissues and to Andreas Bauer for providing the magnificent anatomical drawings. Great thanks to Alexander Kerner for his help with the statistical analysis and to Felix Pirrung for his instructions with the biomechanical trials.

I would also like to extend my sincere thanks to the body donors and their relatives for their selfless decision to donate their bodies for research after their passing.

Abstract in German

Stressinkontinenz ist eine Erkrankung, die meist ältere weibliche Patientinnen betrifft. Es sind jedoch auch junge, weibliche Hochleistungssportlerinnen, die in Sportarten wie Volleyball und Trampolinspringen partizipieren, betroffen. Wiederholtes Springen wird hier als ein kausaler Faktor beschrieben. Die zugrunde liegende Pathophysiologie ist jedoch unvollständig geklärt, insbesondere hinsichtlich des Einflusses umgebender anatomischer Strukturen, inklusive des M. gluteus maximus. Die hier vorliegende Studie hatte zum Ziel, die morphologische Beziehung zwischen dem M. gluteus maximus und dem weiblichen Beckenboden zu untersuchen und in einen mechanischen Zusammenhang zu bringen. Insgesamt wurden 25 Becken Thiel-konservierter weiblichen Körperspenderinnen in Rückenlage präpariert. Zur Beurteilung der mechanischen Eigenschaften einzelner Gewebestränge, die den M. gluteus maximus mit dem Diaphragma urogenitale verbinden, wurden anschließend 20 Gewebestränge hinsichtlich ihrer Versagenslast getestet. Zur weiterführenden Strukturanalyse der bindegewebigen Verbindungen zwischen M. gluteus maximus und dem Diaphragma urogenitale wurden Blockplastinate untersucht und die Erkenntnisse der Präparation validiert. Insgesamt konnten Daten von 49 Beckenhälften von 25 Spenderinnen akquiriert werden. Die Faszie des M. gluteus maximus weist Verbindungen zur Subkutis, zur Faszie des M. sphincter ani externus, zur Faszie des M. obturatorius internus sowie zur Faszie des Diaphragma urogenitale auf. In Bezug auf die Verbindungen zwischen M. gluteus maximus und M. obturatorius internus sowie Diaphragma urogenitale kann diese Verbindung als Fortsetzung der Faszie des M. gluteus maximus betrachtet werden; die Verbindung zwischen M. gluteus maximus und dem Diaphragma urogenitale hatte eine Versagenslast von 23,6 ± 17,3 N. Cramér φ-Analysen zeigten konstante Verbindungen der Faszien, die den M. gluteus maximus mit seiner Umgebung in horizontalen und sagittalen Ebenen verknüpfen. Die hiervorliegende Studie gibt erste Hinweise darauf, dass der M. gluteus maximus mit dem Beckenboden durch Bindegewebsstränge verbunden ist. Während bisherige Forschungsergebnisse darauf hindeuteten, dass die Aktivität des M. gluteus maximus vorbeugend gegen Harnkontinenz wirkt, suggeriert die hier beschriebene morpho-mechanische Verbindung auch eine potenzielle Rolle in der Entstehung der Belastungsinkontinenz. Zukünftige Studien, welche klinische

Bilddaten betroffener Patientinnen mit *in-situ*-Tests kombinieren, könnten weitere Erkenntnisse zum klinischen Einfluss liefern.

Abstract in Englisch

Stress urinary incontinence is a condition that affects not only elderly females but also young female athletes performing in high-impact sports like volleyball and trampolining. Repetitive jumping seems to be an aggravating factor. In general, lax vaginal tissues and weakened supporting structures can lead to stress and urge incontinence. However, the underlying pathophysiology remains incompletely understood, particularly concerning the impact of the surrounding buttock tissues, including the gluteus maximus muscle. The study aimed to investigate the morpho-mechanical relationship between the gluteus maximus and the female pelvic floor.

The study involved the dissection of 25 pelves from Thiel-embalmed female cadavers while in a supine position. The mechanical properties of tissue strands connecting the gluteus maximus to the urogenital diaphragm were assessed in 20 specimens. Plastinates were also evaluated to confirm the dissection findings. In total, data were collected from 49 hemipelves.

The investigation revealed that the fascia of the gluteus maximus extends to the subcutaneous tissue, the fascia of the external anal sphincter, the fascia of the internal obturator, and the fascia of the urogenital diaphragm. This link to the internal obturator and the urogenital diaphragm can be regarded as an extension of the gluteus maximus fascia. The connection between the gluteus maximus and the urogenital diaphragm was able to withstand an average force of 23.6 ± 17.3 N. Cramér φ analyses demonstrated consistent connections of the fasciae linking the gluteus maximus with its surroundings in both the horizontal and sagittal planes.

In conclusion, the study showed that the gluteus maximus is closely linked to the pelvic floor through connective tissue strands and fascial continuations covering the adjacent muscles. While previous research has suggested that the gluteus maximus supports urinary continence, the here-described morpho-mechanical link suggests that it may potentially also play a role in urinary stress incontinence. Future research that combines clinical imaging with in-situ testing may provide additional insights into the clinical implications of these findings.

Publication Disclaimer

SIESS, M., STEINKE, H., ZWIRNER, J. & HAMMER, N. 2023. On the potential morpho-mechanical link between the gluteus maximus muscle and pelvic floor tissues (manuscript submitted for publication). Scientific Reports.

Table of contents

Abbreviations

Bs. *Bulbospongiosus*

Co. *Coccygeus*
Const. *Constant*

EAS. *External anal sphincter*

FGM. *Fascia of gluteus maximus*
FIO. *Fascia of internal obturator*

GM. *Gluteus maximus*

Ic. *Ischiocavernosus*
IO. *Internal obturator*
Is. *Ischium*

LA. *Levator ani*

R. *Rectum*

SCT. *Subcutaneous tissue*
SUI. *Stress urinary incontinence*

TPF. *Superficial transverse perineal muscle*
TPS. *Deep transverse perineal muscle*

U. *U*rethra
UD. *Urogenital diaphragm*

Va. *Vagina*

Table of figures

List of tables

1 Introduction

While urinary incontinence is a condition affecting mostly elderly females, stress urinary incontinence (SUI), which is defined as the involuntary passing of urine under effort or physical exertion (Nambiar et al., 2022), also affects young, nulliparous, female elite athletes. Repeated jumps seem to provoke the onset of SUI, as athletes participating in high-impact sports such as volleyball or trampolining have been reported to have the highest prevalence in recent studies (Nygaard and Heit, 2004, Pires et al., 2020, Gan and Smith, 2023).

Even though it is a common problem, the underlying mechanisms behind urinary incontinence are incompletely understood. Authors described that a laxity of vaginal tissues such as a weakened vaginal wall itself or connective tissues, which invest muscles and ligaments, might give rise to the development of stress and urge incontinence (Petros and Ulmsten, 1990). DeLancey proposed in his “hammock hypothesis” that the urethra is compressed against a “hammock” of structures consisting of the endopelvic fascia, the vaginal wall, the tendinous arch of the pelvic fascia, and the levator ani when the bladder is filled, thereby giving structural support for the urethra (DeLancey, 1994). As a consequence, laxity of these structures could contribute to the onset of SUI (DeLancey, 1994). Generally speaking, the pathophysiology of SUI is a multifactorial process in which weakened supporting structures also contribute to the development.

It is not elucidated to date if the surrounding muscles of the pelvic region, including the gluteus maximus, could additionally weaken these supportive structures under certain circumstances by pulling the pelvic floor laterally and thereby facilitating urinary incontinence.

Opposing to this hypothesis, recent studies have demonstrated a synergistic function of the gluteus maximus. Marques et al. examined the effect of pelvic floor training alone in comparison to strengthening pelvic floor muscles with hip synergistic muscles (gluteus medius, maximus and hip adductor muscles) (Marques et al., 2020). The latter resulted in a significant improvement in urine leakage when compared to the group focusing on just pelvic floor training (Marques et al., 2020). The pelvic floor and gluteus maximus co-activate during walking or running,

however, without complete synchronization (Williams et al., 2022). Here, activation peaked during single-leg support movements (Williams et al., 2022). Functional magnetic resonance imaging and surface electromyography showed changes in the surface area of the ischioanal fossa, gluteus maximus, and levator ani, suggesting a synergistic function (Soljanik et al., 2012). Hence, the authors labeled these three structures the “LFG-complex” (Soljanik et al., 2012).

Functionally, the gluteus maximus appears to influence SUI by providing support. Morphologically, however, research is not entirely conscious of this mechanism. Potential morphological correlates may cross the ischioanal fossa. DeBlok examined the connectives of the ischioanal fossa by dissecting eight female body donors and analyzing plastinates and histological slides. He could illustrate a three-dimensional entity of septa-like fibers that interconnect the gluteus maximus, internal obturator and levator ani (De Blok, 1982a, De Blok, 1982c, De Blok, 1982b). Additionally, DeBlok described different patterns of these septa based on the filling of the rectum, concluding an assisting function by enlarging the width of the bowels (De Blok, 1982c).
Based on the analysis of available literature on this topic, a study focusing on the morpho-mechanical connection between gluteus maximus and the pelvic floor has not been conducted, yet. Consequently, information regarding a potential influence on stress urinary incontinence is needed.

Hence, the present study aimed at assessing the morphological interaction of gluteus maximus and pelvic floor tissues by examining tissue connections on a macroscopic and mesoscopic level in Thiel-embalmed female body donors. Under the condition that such a morphological link could be found, a second goal was to carry out preliminary mechanical testing of this connection.

It was hypothesized that the gluteus maximus is morphologically capable of transmitting force to the pelvic floor via connective tissue fiber strands.

1.1 Topography of the pelvic region

The pelvis serves as the crucial link connecting the trunk, upper limbs, and head to the lower limbs, playing a pivotal role in transmitting the weight of the upper body to the lower extremities while also providing support for the viscera. In the following chapters, the essential anatomical knowledge for the study at hand will be covered.

1.1.1 The pelvic girdle – joints and ligaments

The pelvic girdle presents itself as a ring-like structure that is formed by the two hip bones (composed of the ilium, ischium, and pubis) articulating with each other anteriorly (pubic symphysis), and posteriorly with the sacrum (sacroiliac joint).
In adolescence, the three bones – ilium, ischium, and pubis – are eventually fused together. Initially, however, these three bones are connected to each other via a Y-shaped epiphyseal plate in the acetabulum. In the hip joint, the acetabulum then builds the socket for the head of the femur (Schünke, 2022a). The pelvic girdle obtains improved stability through strong ligamentous support. Multiple ligaments stabilize the sacroiliac joint, which cover the anterior aspect (anterior sacroiliac ligament) and the posterior aspect (posterior sacroiliac ligament) of the sacroiliac joint, as well as the interjacent part (interosseus sacroiliac ligament). By connecting different parts of the sacrum with ischium, the sacrotuberous ligament (sacrum, coccyx, posterior superior iliac spine, and ischial tuberosity) in combination with the sacrospinous ligament (sacrum and ischial spine) provides additional stability for the sacroiliac joint. Joints, supported by strong ligaments, and with reduced mobility, are called amphiarthrosis – to which category the sacroiliac joint belongs. During weight-bearing, the joint is capable of executing small movements (2-4 mm) in an anterior-inferior direction, called nutation (Friedrich et al., 2012, Wong et al., 2022). This is of great importance in preventing fractures of the pelvic girdle when transferring forces exerted by the trunk to the lower limbs (Vleeming et al., 2012). Caudally, the sacrum is connected to the coccyx either as a joint or by synchondrosis. This connection allows passive movement, which is important in the birth process (Friedrich et al., 2012).
Anteriorly, the pubic symphysis completes the pelvic girdle. The two articulating parts of the pubis, covered by hyaline cartilage, work in tandem with a

fibrocartilaginous disc to withstand various types of strain. When bearing weight on both legs, the pubic symphysis withstands drag forces. On a single leg, it experiences shear forces, and during walking, it must endure both compressive and bending forces. The pubic symphysis is supported by two ligaments: one situated superiorly (the superior pubic ligament) and the other found inferiorly (the inferior pubic ligament) (Friedrich et al., 2012). As mentioned earlier, the acetabulum and the femoral head together create the hip joint. A cartilaginous labrum covers this ball-and socket-joint to enhance stability. Robust ligaments and a strong capsule restrict motion in all directions to prevent dislocation of the femoral head. Among these, the iliofemoral band, one of the strongest ligaments of the human body, extends from the anterior inferior iliac spine to the intertrochanteric line and can be subdivided into medial and lateral parts. During adduction and external rotation, the lateral part tightens, while the medial part prevents hyperextension of the hip joint. The pubofemoral ligament, originating from the superior ramus of the pubic bone and attaching at the intertrochanteric line, restricts extension, abduction, and external rotation. The ischiofemoral ligament, the third ligament, tenses during internal femur rotation, extension, or abduction. With its origin at the dorsal part of the acetabulum and the insertion site at the trochanteric fossa and the iliofemoral ligament, the ischiofemoral ligament extends spirally around the femoral neck (Friedrich et al., 2012).

1.1.2 Hip muscles and the pelvic floor

This chapter delves into the muscles that were important during the dissections and for the data acquisition. Specifically, the gluteus maximus, internal obturator, levator ani, external anal sphincter, and the urogenital diaphragm with its different parts will be covered.

1.1.2.1 Gluteus maximus and the internal obturator

The gluteus maximus originates from the lateral aspect of the sacrum’s dorsal part, the posterior part of the ilium posteriorly to the gluteal line, the thoracolumbar fascia, and the fascia of the gluteus medius. It also emerges from the deep fibers of the sacrotuberous ligament. The cranial muscle fibers insert into the iliotibial tract, while the caudal part attaches to the femur at the gluteal tuberosity. With its two insertion sites, the gluteus maximus can conduct abduction (through its cranial

fibers) as well as adduction (through its caudal fibers) in the hip joint. In tandem, the two parts work to induce retroversion and external rotation. Furthermore, the gluteus maximus plays a crucial role in stabilizing the hip joint in both the sagittal and frontal planes, and through its connection to the iliotibial tract, it contributes to the extension of the knee (Friedrich et al., 2012, Schünke, 2022a). The internal obturator originates from the inner side of the obturator membrane, along with the surrounding bones, and inserts in the trochanteric fossa of the femur. Its tendon fuses together with the tendons of the superior gemellus and inferior gemellus muscles to form the triceps coxae muscle. Together, they facilitate external rotation in the extended and abduction in the bent hip joint (Schünke, 2022a, Friedrich et al., 2012).

1.1.2.2 The pelvic floor

The pelvic floor serves as the inferior boundary to the pelvic cavity and consists of two partially overlapping muscular plates through which the vagina and rectum pass in the female pelvis. These plates function as both supporting structures and muscles important for continence. Each of the plates consists of multiple muscles:

Pelvic diaphragm	Urogenital diaphragm
- Levator ani - Coccygeus - External anal sphincter	- Deep and superficial transverse perineal muscle - Ischiocavernosus - Bulbospongiosus - External urethral sphincter

Table 1: Overview of the muscles building the pelvic diaphragm and the urogenital diaphragm.

The levator ani spans between both sides of the lesser pelvis and constitutes a significant part of the pelvic floor. It consists of three components: the puborectalis, pubococcygeus, and iliococcygeus. The puborectalis extends from the superior ramus of the pubis in proximity to the pubic symphysis posteriorly to the anorectal junction, where it intertwines with the external anal sphincter. Due to this sling-like morphology, the puborectalis creates the anorectal angulation and provides support for the rectum, vagina, bladder, and urethra by pulling them ventrally (Friedrich et al., 2012, Schünke, 2022a, Azpiroz et al., 2005, Strohbehn, 1998). The pubococcygeus muscle, like the puborectalis, originates from the superior

ramus of the pubic bone, situated laterally to the puborectalis. It inserts at the anococcygeal ligament and the coccyx. The iliococcygeus, emanating from the tendinous arch of the internal obturator, fans out and attaches to the pubococcygeus. Collectively, these three muscles, known as the levator ani, enclose a significant portion of the pelvic cavity, ensuring the stability of pelvic organs (Schünke, 2022a, Friedrich et al., 2012). As previously mentioned, the puborectalis interlaces with the external anal sphincter, which is an annular muscle extending from the perineal body to the anococcygeal ligament. This muscle is made up of three layers: a subcutaneous, a superficial, and a deep layer. It covers the anal canal, beginning at the skin and extending cranially for about three to four centimeters. It is worth noting that various concepts exist in the literature regarding the morphology of the external anal sphincter (Schünke, 2022a, Friedrich et al., 2012, Enck et al., 2005). In contrast to the funnel-shaped pelvic diaphragm, the urogenital diaphragm is a horizontally oriented plate located caudally to the pelvic diaphragm. The muscles in this region lie in two different compartments: the superficial perineal pouch and the deep perineal pouch. While the deep transverse perineal muscle and the external urethral sphincter lie in the deep perineal pouch, the superficial transverse perineal muscle, the ischiocavernosus, and the bulbospongiosus are found in the superficial perineal pouch (Schünke, 2022a, Friedrich et al., 2012). The deep transverse perineal muscle spans between the inferior ramus of the pubis and the ischial ramus of each side, converging at the perineal body and providing coverage for the vagina and the urethra. In comparison to the male pelvic floor, this muscle is usually weaker in women as the vagina passes through it. Some fibers of this muscle encircle the urethra, forming what is known as the external urethral sphincter. Originating from the ischial tuberosity, the superficial transverse perineal muscle inserts at the perineal body. In many cases, this muscle is less developed. The ischiocavernosus muscles on each side extend from the ramus of the ischium to the crus of the clitoris, aiding in clitoral erection during sexual arousal. The bulbospongiosus covers the lateral part of the vaginal orifice, assisting in vaginal contraction (Schünke, 2022a, Friedrich et al., 2012). In summary, the pelvic floor, by enveloping the caudal part of both the pelvic and abdominal cavity as a cohesive unit, provides essential stability for the pelvic organs, including the urethra/bladder, vagina, and rectum, as well as the

abdominal organs. Moreover, since these organs traverse different parts of the pelvic floor, the adjacent muscles play a crucial role in regulating the diameters of these openings, thereby contributing to their continence function (Schünke, 2022a, Friedrich et al., 2012).

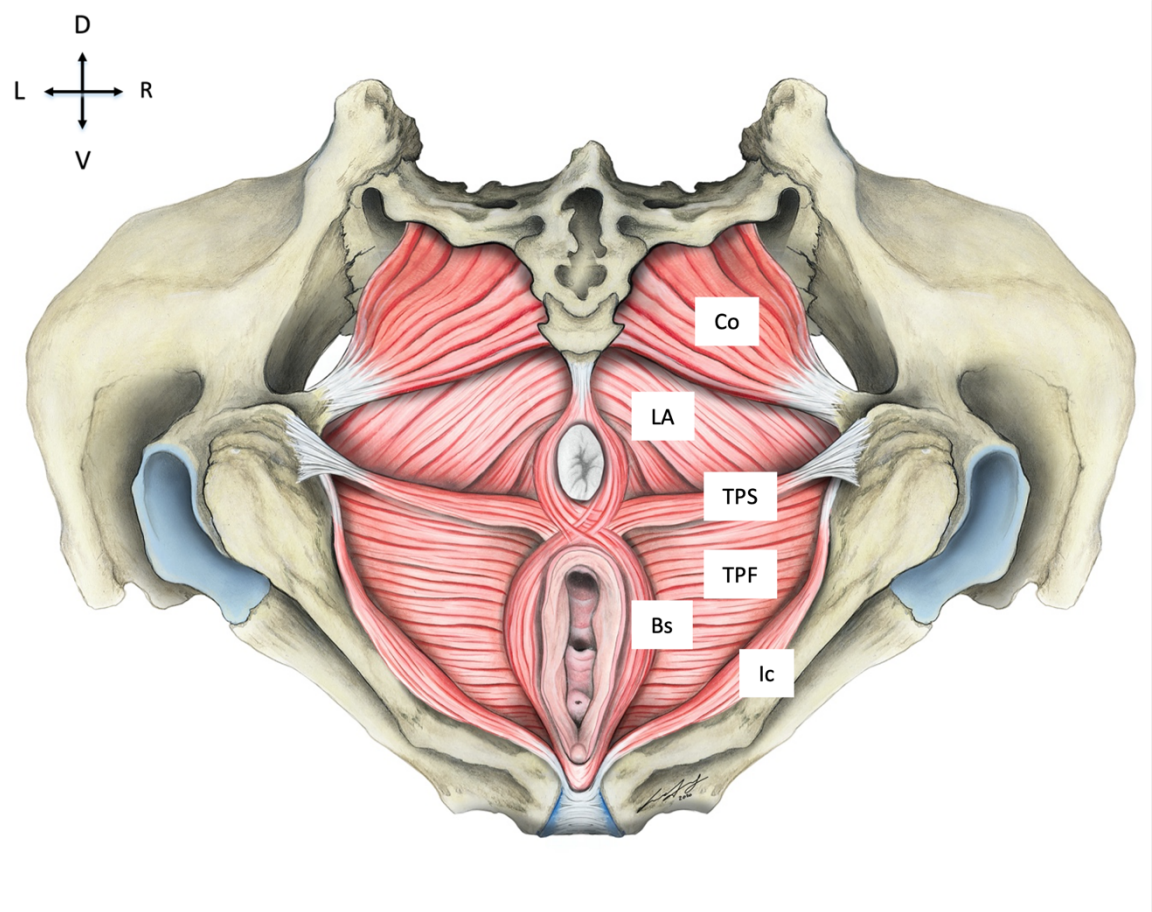

Figure 1: Overview of the female pelvic floor. Co – Coccygeus, LA – Levator ani, TPS – Deep transverse perineal muscle, TPF – Superficial transverse perineal muscle, Bs – Bulbospongiosus, Ic – Ischiocavernosus. Curtesy Andreas Bauer, Medical University of Graz.

1.1.3 Fascial topography of the pelvic floor

The pelvic floor is interconnected by multiple fasciae, creating a complex network that defines three distinct spaces: the superficial perineal pouch, the deep perineal pouch, and the ischioanal fossa (Roberts et al., 1964, Schünke, 2022a). The pelvic diaphragm is enveloped by both the inferior and superior fascia of the pelvic diaphragm. On its lateral boundary, the internal obturator, along with its fascia, forms one of the borders of the ischioanal fossa. Moving caudally, the superior and inferior fascia of the urogenital diaphragm encase the urogenital diaphragm. The deep perineal pouch lies in-between these fascial folds and contains the deep

transverse perineal muscle, external urethral sphincter, parts of the urethra, the Bartholin´s gland (women) or Cowper´s gland (men) and pudendal neurovascular bundles. Inferiorly to this, the superficial perineal pouch contains the erectile soft tissues in females and males, as well as the bulbospongiosus and ischiocavernosus muscles. Once again, this pouch also contains pudendal neurovascular bundles. The inferior fascia of the urogenital diaphragm forms the cranial boundary, while the superficial perineal fascia serves as the caudal boundary, and the superficial transverse perineal muscle forms the dorsal boundary (Schünke, 2022a). In close proximity, the gluteal suspension system originates from the ischial tuberosity and the sacrotuberal ligament. Laterally, it fuses together with the iliotibial tract, while superiorly, parts of the gluteal suspension system extend to the gluteal fascia and the aponeuroses of the gluteal muscles (Steinke, 2018).

1.1.4 The ischioanal fossa

The ischioanal fossa takes on the shape of a three-sided pyramid, with its apex near the pubic bone and the base oriented dorsolaterally. It is bordered laterally by the obturator fascia, which covers the obturator internus; medially by the inferior fascia of the pelvic diaphragm, covering the levator ani and the external anal sphincter; and caudally by the ischial tuberosity. The gluteus maximus forms the dorsal margin. The foremost portion is sometimes called the “pubic recess”, which is located between the urogenital diaphragm and the levator ani muscle. Along the lateral border, a duplication of the obturator fascia creates the pudendal canal, a tunnel-like structure through which the pudendal nerve and the internal pudendal vessels travel ventrally alongside the internal obturator. As they make their way towards the urogenital diaphragm and the genitals, the neurovascular bundles send branches transversely through the ischioanal fossa to the external anal sphincter and the perineal skin. These branches are known as the inferior rectal nerve and the inferior rectal vessels. Fatty tissue and connective tissue fill the fossa, allowing the rectum to extend during defecation (Friedrich et al., 2012). Abscesses and anorectal fistulae can be located in the ischioanal fossa (Morgan, 1949).

1.1.5 Viscera

1.1.5.1 Rectum and anal canal

Continuing from the sigmoid colon, the rectum extends for a length of approximately 15cm to reach the anal canal. Featuring two s-shaped flexures in a sagittal plane, the morphology of the rectum does not adhere to its name. The first, upper one, known as the sacral flexure, follows the pelvic contour of the sacrum. Upon reaching the perineal membrane, the rectum recurves anteriorly, forming the second curve, called the perineal flexure. With its sling-like morphology, the puborectalis contributes to this angulation (Wang and Wiseman, 2023, Friedrich et al., 2012, Schünke, 2022b). Within the rectum, three transverse mucosal folds can be present, with the middle one consistently present and referred to as Kohlrausch´s valve. This fold is situated at a distance of approximately 6-7 cm from the anus and can be reached by a finger during examination. Consequently, rectal carcinomas lying below Kohlrausch´s valve may be palpable during a digital rectal exam (Friedrich et al., 2012, Schünke, 2022b). The rectal ampulla lies between this fold and the anorectal junction. With many stretch receptors and usually being unfilled, the rectal ampulla serves as an indicator for the urge to defecate. As the ampulla fills to a certain amount, visceral afferences send signals to the sensory cortex to initiate defecation promptly (Schünke, 2022b). The final segment of the gastrointestinal tract is the anal canal, which exhibits distinct histological regions. The cranial part features columnar epithelium, followed by a transition zone containing columnar, stratified squamous, or transitional epithelium. The caudal section consists of a squamous epithelium that merges with the perianal skin (Barleben and Mills, 2010).

1.1.5.2 Vagina

Vagina and uterus lie ventrally to the rectum, enclosing the rectouterine pouch, also known as the pouch of Douglas, which constitutes the deepest part of the female peritoneal cavity. On the longitudinal axis, the vagina faces cranially and dorsally. In a transverse section, the vagina exhibits an H-shaped structure with its anterior and posterior walls in close contact. Both the vagina and urethra pass through the pelvic floor in close proximity to each other. In this region, the deep

perineal muscle sends out muscle fibers that encircle both structures. In the case of the urethra, these fibers are called the external urethral sphincter (Schünke, 2022b, Friedrich et al., 2012).

1.1.5.3 Urinary bladder and the female urethra

The urinary bladder is the most ventral viscus in the pelvis and lies underneath the uterus when empty. In healthy individuals, the bladder has a maximum capacity of 500 to 700 ml of urine, with the urge to urinate typically arising at 150 to 200 ml. During pregnancy, this urge can occur even earlier as the uterus compresses the bladder from above. The bladder consists of a body, a fundus, and an apex. The urine from both ureters empties into the fundus from dorsolateral positions. It then flows ventrocaudally towards the vesical cervix, where the bladder transitions to the urethra. The trigone of the urinary bladder, positioned between the ureter orifices and the internal urethral orifice, is a crease-free mucosal region as the underlying muscles here adhere to the mucosa (Sam et al., 2023, Schünke, 2022b, Fritsch and Kühnel, 2018). Morphologically, the vesical wall is primarily composed of smooth muscle fibers, forming the vesical detrusor. This muscle features three layers oriented in different planes: the outer and inner longitudinal layers, and a circular layer in between. The vesical detrusor then continues into the vesical sphincter. Together, they work as a unit to store and pass urine. During the filling stage, the detrusor muscle relaxes while the vesical sphincter contracts. Conversely, during micturition, this pattern obverts, with the detrusor contracting to force urine outflow through the urethra. Additionally, the longitudinal muscle of the urethra aids in micturition by shortening the urethra and enlarging the urethral orifice. The contraction of this muscle initiates micturition (Sam et al., 2023, Schünke, 2022b, Fritsch and Kühnel, 2018).

1.1.6 Neurovascular anatomy of the pelvic floor

The pudendal nerve originates from three rami of the sacral plexus, spanning from S2-S4. Throughout its path, the nerve exits the pelvis via the greater sciatic foramen, briefly traverses the gluteal region, and reenters the pelvic region via the lesser sciatic foramen. It continues along the lateral wall of the ischioanal fossa, covered by a connective tissue sheath stemming from the fascia of the internal obturator muscle. This tunnel-like structure is referred to as the pudendal canal or

Alcock canal (Kinter and Newton, 2023). Within this canal, the inferior rectal nerve branches off, piercing through the connective tissue sheath and traversing through the fat tissue of the ischioanal fossa to reach the external anal sphincter. As the pudendal nerve exits the pudendal canal, it gives rise to the perineal nerve, which innervates the skin (superficial branch) and pelvic floor muscles (muscular branch) of both the superficial and deep perineal pouches. The terminal branch of the pudendal nerve innervates the penile or clitoral shaft and glans and is, therefore, known as the dorsal nerve of the penis or clitoris. This nerve also plays a role in facilitating erections by communicating with the cavernous nerve, which promotes blood flow to the erectile tissues (Kinter and Newton, 2023). The anterior division of the internal iliac artery sends off the internal pudendal artery as one of two terminal branches. The internal pudendal artery then passes through the infrapiriform foramen and reenters through the lesser sciatic foramen, subsequently following the course of the pudendal nerve and the internal pudendal vein. These structures travel within the pudendal canal (Zaunbrecher et al., 2023, Schünke, 2022a).

1.2 Physiology of urinary continence

Urinary continence is a complex interplay of multiple pelvic floor muscles. It involves two sphincter muscles: one located at the bladder (internal sphincter), and the other found at the urethra, known as the external sphincter. The external sphincter features an inner smooth muscle, arranged in a circular fashion, and an outer part made of striated muscle, together forming a horseshoe shape. The lateral muscle fibers yield attachments to the fascia of the levator ani, hence suggesting the need for an intact function of the levator ani to provide sufficient closing pressures (Wallner et al., 2009, Schünke, 2022b). From an anatomical perspective, the stress continence control system can be subdivided into the urethral support system and the sphincteric closure system (Ashton-Miller et al., 2001). Externally, structures such as the anterior vagina, the endopelvic fascia, the tendinous arch of the pelvic fascia, and the individual muscles contributing to the levator ani provide support for the urethra (DeLancey, 1994). Internally, the sphincteric closure system consists of the urethral muscles (striated and smooth muscle) and the vascular elements located in the submucosa. These three

components seem to equally contribute to the intraurethral closing pressure at rest. The interaction of these systems, which provides for an appropriate closing pressure, as well as the timing of pelvic floor contraction, result in urinary continence (Ashton-Miller et al., 2001).

1.3 Urinary stress incontinence in female elite athletes

Stress urinary incontinence is characterized by the unintentional release of urine during physical exertion or effort (Nambiar et al., 2022). While urinary incontinence is commonly associated with elderly females, recent research indicates a substantial occurrence of SUI among young, nulliparous female high-performance athletes. Specifically, female athletes engaged in high-impact sports like volleyball or trampolining appear to have the highest prevalence of SUI, with repeated jumps thought to be a potential triggering factor for its onset. (Nygaard and Heit, 2004, Pires et al., 2020). One study reported that up to 80% of female elite trampolinists experienced SUI (Eliasson et al., 2002). Yet, the exact pathophysiology remains incompletely elucidated to this date. There are two controversial theories about the effects of physical activity on the pelvic floor. One theory suggests that strenuous exercise leads to muscular fatigue of the pelvic floor muscles. In this study, ninety minutes of strenuous physical activity resulted in lower voluntary vaginal contraction pressure, which can be indirect evidence of pelvic floor muscle fatigue (Casey and Temme, 2017). On the other hand, exercise may strengthen the pelvic floor tissues as increased intra-abdominal pressure stimulates a simultaneous pre-contraction of these structures, possibly leading to muscular strengthening (Bo, 2004).

1.4 The aim of this study

The objective of the given study was to investigate the morphological connection between the gluteus maximus and pelvic floor muscles in Thiel-embalmed female body donors, evaluating tissue connections at both a macroscopic and mesoscopic scale. Additionally, the study aimed to perform initial mechanical tests to determine if such connections could be demonstrated.

The hypothesis underlying this investigation was that the gluteus maximus holds the capability to exert force on the pelvic floor through strands of connective tissue.

2 Material and Methods

The study was conducted after receiving approval from the Ethics Committee of the Medical University of Graz, with protocol number 32-377 ex 19/20. Between July 2020 and April 2022, pelves from 27 female body donors who had provided prior consent for the use of their bodies for medical education and scientific research were dissected. Biomechanical testing was subsequently performed in June 2022. All specimens were preserved using the Thiel embalming technique (Thiel, 1992b, Thiel, 2002).

2.1 Thiel embalming technique

The Thiel embalming method, renowned for preserving both optical and tactile tissue properties, is employed for educational dissection and scientific research in Graz. Walter Thiel's extensive experience, spanning 977 body donors over 30 years by the time of his 1991 publication, underlines this preservation technique. The process involves various solutions administered throughout the vascular, gastrointestinal, respiratory, and central nervous systems. Subsequently, the body remains in an additional solution for six months (Thiel, 1992b). After a decade of refining this technique, Thiel published an updated version in 2001, focusing on improved preservation solution compositions and comprehensive brain conservation. The solutions now incorporate the following ingredients:

- Stock solution I: 100 liters of hot tap water, 3kg of boric acid, 30 liters of mono propylene glycol, 20kg of ammonium nitrate and 5kg of potassium nitrate
- Stock solution II: 10 liters of mono propylene glycol and 1 liter of 4-chlorine-3-methyl phenol
- Infusion solution + intestines solution: 12 liters of stock solution I, 0.5 liters of stock solution II, 0,6kg sodium sulphite, 0,45 liters of morpholine, 0,5 liters of formalin, and 2 liters of ethyl alcohol
- Solution for preservation in a bin: 91 liters of hot tap water, 3kg boric acid, 10 liters of mono propylene glycol, 10kg ammonium nitrate, 5kg potassium nitrate, 9 liters of ethyl alcohol, 2 liters of formalin, 7kg sodium sulphite, and 2 liters of stock solution II
- Brain + spinal cord solution: 40 liters of tap water, 45 liters of ethyl alcohol, and 15 kg of formalin (Thiel, 2002, Wilke et al., 2011).

2.2 Plastination

The plastination technique, developed by Gunther von Hagens, employs reactive polymers to preserve anatomical specimens. Plastination offers a unique advantage by allowing the examination of structures in the "mesoscopic area." Transparent body slices enable the study of topography within its physiological context. Various polymers have been used for plastination, with silicone (S10), epoxy (E12), and polyester (P40) being among the most well-known (Sora et al., 2019).

The plastination process involves several key steps:

1. Fixation and coloring:

One common fixation method involves the use of formalin, with concentrations typically ranging from 1% to 20%. Minimizing fixation times preserves the specimen's natural color. If necessary, colored epoxy resin can be intravascularly applied.

2. Dehydration:

Dehydration involves replacing water with an organic solvent. This is achieved by immersing the material in solutions with gradually increasing concentrations of the organic solvent. This technique minimizes the risk of shrinking the plastinate. Alternatively, freezing substitution can be used. Commonly employed solvents include alcohol or acetone (freeze substitution).

3. Forced Impregnation:

Forced impregnation is a crucial step in plastination, where a reactive polymer like silicone, epoxy resin, or polyester resin replaces the organic solvent used for dehydration. A vacuum is essential for this process, creating a gradient that facilitates the infusion of the reactive polymer due to differences in vapor pressure and boiling points between the two substances.

4. Induration:

The hardening process varies depending on the type of polymers used. It may involve gas curing (silicone), natural hardening at room temperature, or light exposure (von Hagens, 1985).

The validity of the experimental data was confirmed through examination of a plastinate collection provided by Hanno Steinke from Leipzig. In summary, fresh-frozen blocks were first sliced, followed by freeze substitution in acetone and subsequent vacuum embedding in epoxy resin, as described above by von Hagens (von Hagens, 1985). Additionally, specific plastinates were stained using the PAS method to differentiate between various collagen types, each exhibiting distinct staining characteristics (Steinke et al., 2018).

2.3 Exclusion criteria and study population

The exclusion criteria for the present study comprised any pre-existing alterations of pelvic floor tissues, like surgeries in the perineal area, neoplasms of the pelvic floor, the ischioanal fossa or traumatic injuries to the pelvic tissues. Only female body donors were included because of the sample size of 25 body donors. On average, the body donors were 84±10 years old.

	Average	Maximum	Minimum
Age in years	83.8	98	57

Table 2: Age distribution within the study population.

2.4 The approach to the ischioanal fossa

Analyzing previously dissected body donors, prepared during one of the curricular dissecting courses, contributed to the development of the dissection approach, facilitating a better topographical understanding of the pelvic floor region. Specimens, which had undergone dissection at the midpoint of the femur and the middle of the thoracic spine prior to the trials, were examined while in a supine position. Despite the removal of numerous fibers within the fossa, particularly the ventral ones, the preparations revealed connections originating from the gluteus maximus, attaching it to the internal obturator and the levator ani. Elevation of the gluteus maximus upwards resulted in a synchronous pelvic floor movement. The injection of a mass consisting of dextrin, latex, and lead tetroxide, a method also

documented by Walter Thiel (Thiel, 1992a), made arteries within the soft tissue fibers visible. Due to the initial uncertainty about the optimal approach to the ischioanal fossa at the outset of the dissections, various options were explored. Consequently, the initial two dissections were considered exploratory in nature, with the objective of defining the most suitable approach to the ischioanal fossa while focusing on preserving physiological anatomy and obtaining detailed anatomical knowledge. Notably, these two specimens were excluded from the subsequent sample size.

Eventually, the final approach comprised four key steps:

1. Skin Incision: The iliac crest was the landmark for determining the correct height of the transverse cut, extending from one side of the specimen to the other. Longitudinal cuts followed on both sides, terminating approximately at the midpoint of the femur. In cases where the lower extremities had been removed at mid-femoral, the length of the horizontal cut was limited. However, in all instances, the length proved to be adequate, and it was never a reason for exclusion. A second transverse incision to the middle of the thigh marked the completion of the first step of the approach to the ischioanal fossa.
2. Preparation of the gluteal and thigh fascia: Following the identification of the fascia of the gluteus maximus at the craniolateral border of the skin flap, the preparation began at this corner and extended to the muscle's medial border. Resection of more robust adhesions between subcutaneous tissue and fascia occasionally necessitated the use of scissors or a scalpel. However, applying tension and gentle pressure to the index finger in the described direction typically sufficed to separate the fascia from the subcutaneous tissue. Upon reaching the ischial tuberosity region, the preparation from the craniolateral side ceased, and dissection of the hamstring fascia commenced. The second step concluded once the origin of the hamstrings at the ischial tuberosity became visible.
3. Opening the ischioanal fossa: The ischioanal fossa was opened by inserting a finger in the cranial part, near the sacrum, and gently separating the soft connective tissue and adipose tissue. Some of these connections along the medial border of the gluteus maximus were dissected sharply to enlarge the

opening and optimize visibility. Paper towels were used to reduce fluid and fat content in the fossa. At the end of this step, the following structures within the ischioanal fossa were identifiable: the internal obturator muscle, levator ani muscle, external anal sphincter muscle, urogenital diaphragm, pudendal canal, inferior rectal artery and veins, and the inferior rectal nerve.

4. Preparation of the urogenital diaphragm: This step commenced by locating the inferior ramus of the ischial bone, which served as a landmark for the subsequent dissection. Initially, the urogenital diaphragm was prepared in a caudal to cranial direction. To ensure the preservation of the structural integrity of the urogenital diaphragm, the connective tissue connecting the inferior ramus of the ischial bone and the skin of the inner thigh was dissected in layers, proceeding from dorsal to ventral and from caudal to cranial. The resulting connective tissue flap was resected at the thigh side until the ischiocavernosus, and the urogenital diaphragm became visible. Subsequently, the dense connections between the gluteal fascia and subcutaneous tissue in the ischial tuberosity region were dissected cautiously, stopping once the bottom border of the gluteus maximus appeared. Throughout this step, the ischioanal fossa was cautiously cleared of redundant connective and adipose tissues. This allowed for an assessment of the ischioanal fossa's topography and data acquisition through the completion of the case report form (see attachment). Photographs played a vital role in documenting results and tracking the progress of preparatory skills developed during the dissections.

2.5 Sagittal and transverse planes

To ensure reproducibility and a high level of standardization, three transverse and three sagittal planes were determined for the subsequent data collection.

Level	Transverse plane	Sagittal plane
1st	Skin	Medial border of the ischial tuberosity/internal obturator
2nd	Pudendal canal/upper border of the obturator internus	Ischioanal fossa
3rd	Deep ischioanal fossa/cranial to the pudendal canal	Pubic symphysis / pelvic diaphragm / urogenital diaphragm

Table 3: Transverse and sagittal planes (Siess et al., 2023).

In the following, the planes are displayed schematically.

Horizontal/ transverse planes:

- 1st plane: skin level plane

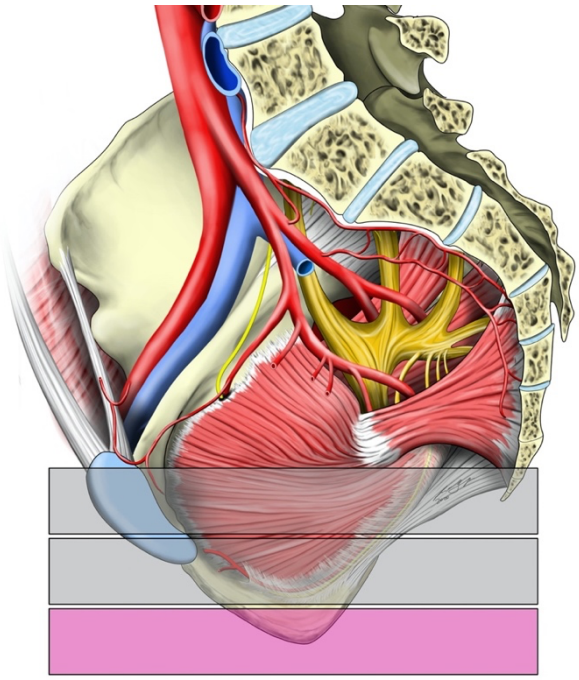

Figure 2: Skin level plane. Curtesy Andreas Bauer, Medical University of Graz.

- 2nd plane: pudendal canal/upper border of the internal obturator

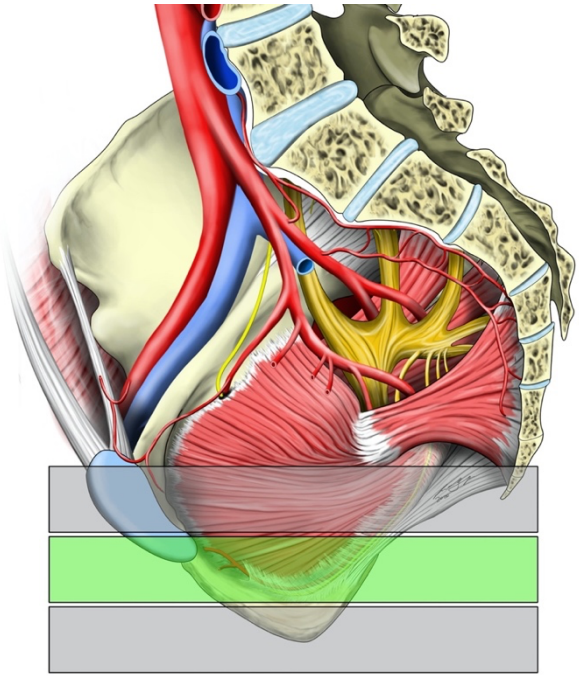

Figure 3: Plane at the height of pudendal canal/upper border of the internal obturator. Curtesy Andreas Bauer, Medical University of Graz.

- 3rd plane: deep ischioanal fossa/cranial to the pudendal canal

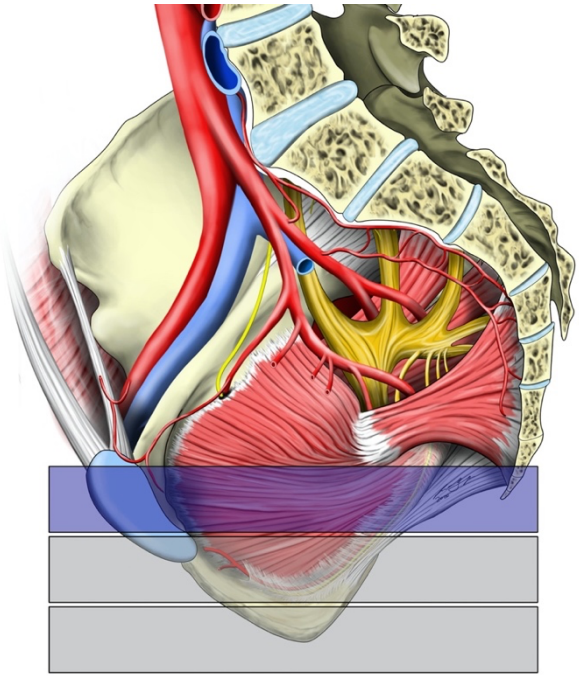

Figure 4: Plane at the level of the deep ischioanal fossa/cranial to the pudendal canal. Curtesy Andreas Bauer, Medical University of Graz.

Sagittal planes:

- 1st plane: medial border of the ischial tuberosity/internal obturator

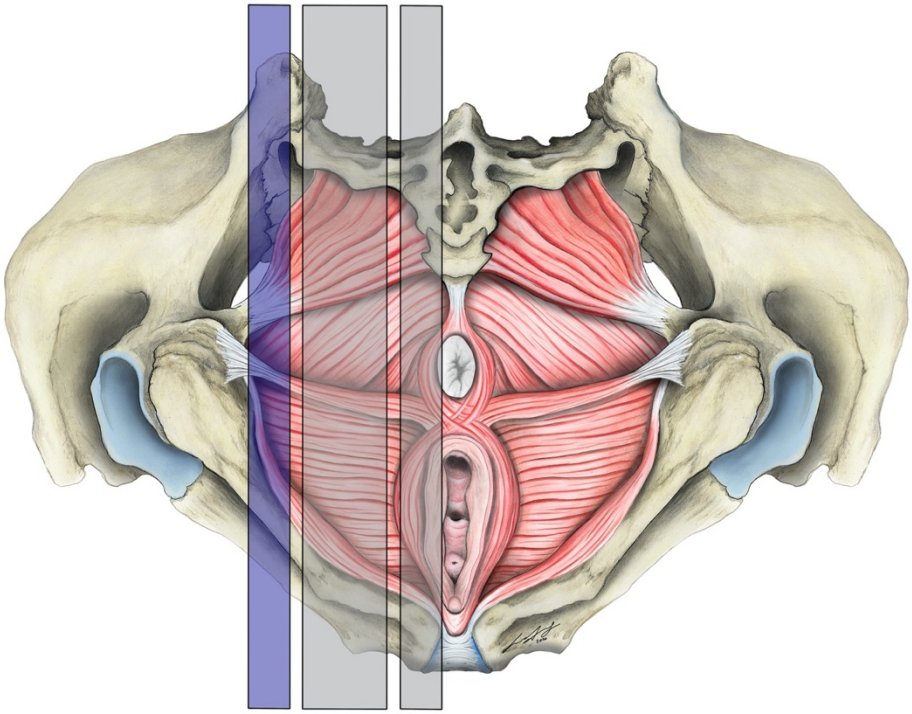

Figure 5: Level of the medial border of the ischial tuberosity/internal obturator. Curtesy Andreas Bauer, Medical University of Graz.

- 2nd “area” ischioanal fossa

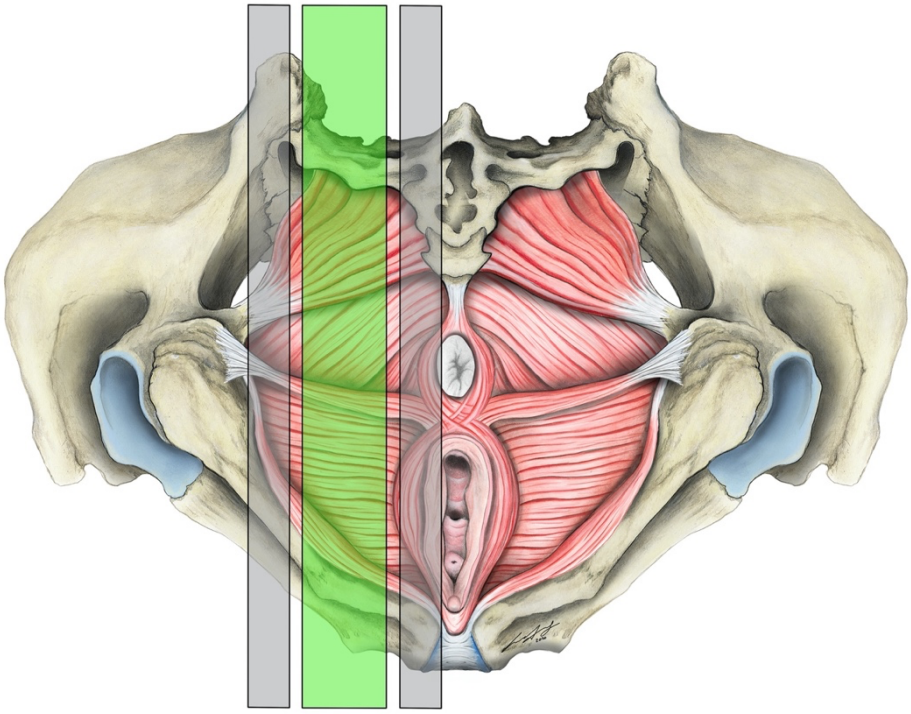

Figure 6: Area of the ischioanal fossa. Curtesy Andreas Bauer, Medical University of Graz.

- 3rd plane: pubic symphysis/pelvic diaphragm/urogenital diaphragm

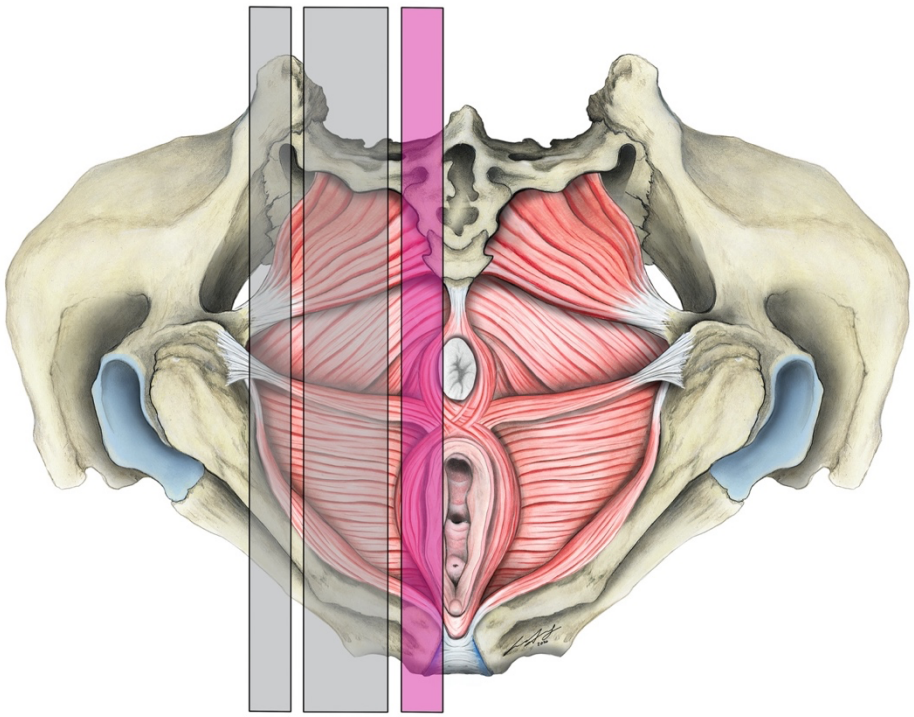

Figure 7: Level of the pubic symphysis/pelvic diaphragm/urogenital diaphragm. Curtesy Andreas Bauer, Medical University of Graz.

2.6 Data collection

Following the dissection, data acquisition was conducted by completing the case report form (see attachment) to document the dissection process and outline the approximate course of the fibers within the ischioanal fossa. These drawings were self-conceptualized using an iPad Air. Subsequently, the gathered data was transferred into an Excel spreadsheet.

The following parameters were acquired:

- Connections: identifying which muscles or fasciae are connected at the given plane.
- Arrangement: determining whether the fibers are present bilateral or unilateral.
- Symmetry: assessing symmetry by pulling the skin flap contralaterally until tension of the urogenital diaphragm.
- Insertion angle: sharp, flat, or perpendicular, with assessment conducted in the same position as mentioned in the point above.
- Quantity of fibers: the number of fibers observed.
- Composition: description of whether the connections consist of connective tissue, neurovascular bundles, or muscle tissue.

2.7 Collecting samples

Biomechanical testing was conducted using twenty tissue samples obtained from ten individuals, with an average age of 79±12 years, ranging from a minimum of 57 years to a maximum of 94 years. The connection between the greater gluteal muscle and the urogenital diaphragm might potentially impact the development of stress urinary incontinence. Consequently, the decision was made to perform biomechanical testing on this connection. Sample collection involved the removal of approximately 15mm of the greater gluteal muscle and 15 mm of the urogenital diaphragm using a scalpel. Initially, the gluteus maximus was resected, starting dorsally and extending towards the gluteus medius. The incision continued alongside the inferior ramus of the ischial bone, adjacent to the ischiocavernosus muscle. Maintaining contact with the bone was essential to prevent damage to the connection. Pulling the resected portion of the gluteus maximus dorsally and contralaterally facilitated the detachment of the tissue from the bone. Upon

reaching the urogenital diaphragm, scissors were used to make the final cut and obtain the sample. These samples were subsequently placed in a container filled with Thiel solution. Due to the substantial variation in the available tissue for resection, a standardized sample size or cross-section area could unfortunately not be guaranteed. However, all samples achieved the required length of 40mm to fit the clamping table.

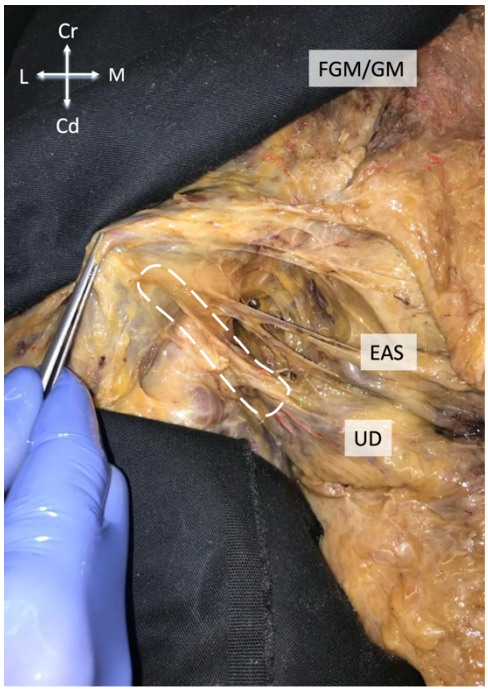

Figure 8: Ischioanal fossa on the left side of a body donor in a supine position. Gluteus maximus is lifted dorsally. The white dashed line represents the approximate course of sample retrieval for the biomechanical testing. EAS – External anal sphincter; FGM – Fascia of gluteus maximus; UD – Urogenital diaphragm (Siess et al., 2023).

2.8 Biomechanical testing

The setup for the biomechanical testing consisted of a universal testing machine by Z020 (Zwick-Roell AG, Ulm, Germany). The following parts were utilized for the biomechanical testing: straight scissors, a size 3 scalpel, two forceps, a preparation table, four clamps (equipped with sharp pyramids), and two holder arms. Notably, the preparation table, clamps, and holder arms were 3D-printed. The testing protocol is detailed below.

Testing Protocol:

Step 1: Preparation of the sample

- The samples underwent trimming to match the length of the preparation table using the scalpel and scissors (length: 40mm, width: 10mm, clamp-to-clamp distance: 20mm).

Step 2: Mounting the sample

- For this step, the components included a preparation table, four clamps, and two holder arms.
- A clamp was positioned on each side of the table. Subsequently, the sample was placed on top and securely fastened by affixing the remaining two clamps to the tissue sample. These clamps were then compressed by hand and secured within the holder arms.

Step 3: Conducting the mechanical testing

- The holder arms were inserted above the gripping jaw inserts of the testing machine. Following this, the pneumatic clamps were engaged with a pressure of 29 psi.
- The mechanical testing process was initiated and monitored via the computer interface. A preconditioning of five cycles up to 1 N commenced the testing (velocity 0.1 mm/sec). The trials ceased when the maximum force fell below 1 N.
- Testing concluded with the disengagement of the pneumatic clamps and the removal of the tissue sample.

The process and the materials used in the testing are based on a technique as stated elsewhere (Scholze et al., 2020).

2.9 Statistical evaluation

The data were analyzed using Prism version 9 (GraphPad Software Inc., La Jolla, CA, USA), SPSS version 28 (IBM, Armonk, VA, USA) and Microsoft Excel version 16.49 (Microsoft Corp., Armonk, NY, USA). Normal distribution was assessed using Pearson´s chi-squared test. Fisher's exact test and Cramér's φ correlations were determined to compare categorical items between symmetry and connections. φ values of 0.1, 0.3 and 0.5 were considered small, medium, and large effect sizes. P-values ≤ 0.05 were considered statistically significant (Ellis, 2010).

3 Results

3.1 *Study population*

Two pelves were dissected for trialing purposes; hence, the study population comprised 50 hemipelves in total. However, one side had to be excluded due to extensive scar tissue affecting the topography at the medial border of the gluteus maximus and at the transition to the ischioanal fossa. Consequently, the final sample size consisted of 49 hemipelves from female body donors.

Both sides included	One side included	Total sides
24	1	49

Table 4: Included sides.

3.1.1 Dissection

3.1.2 Horizontal planes

Skin level plane:

In all 25 dissected specimens, the fascia of the gluteus maximus was connected to the subcutaneous tissue. This connection could be found bilaterally in 24 body donors, as one side was excluded in one specimen. In 21 cases, the connection appeared symmetrical; in three cases it was asymmetrical; and in one case, symmetry could not be evaluated. These connections between the gluteus maximus fascia and the subcutaneous tissue covering the ischioanal fossa exhibited a fatty tissue-like structure. Around the ischial tuberosity region, these connections transitioned in structure from fatty tissue-like to dense, skin-like consistency.

Connections	***Arrangement***	***Symmetry***	***Insertion angle***
FGM + SCT	Bilateral	Symmetrical	Not applicable
25	24	21	
	Not applicable	Asymmetrical	
	1	3	
		Not Applicable	
		1	

Table 5: Detailed acquired data at the skin-level plane.

The connection consisted of connective tissue without macroscopically visible muscle fibers and neurovascular bundles in 25 cases.

Composition		
Connective tissue	Muscle fibers	Neurovascular bundles
25	0	0

Table 6: Composition of the connections at the skin-level plane.

Pudendal canal plane:

In this plane, the fascia of the gluteus maximus laid on top of the fascia of the internal obturator in all 25 cases. Consequently, the inferior rectal vessels and the inferior rectal nerve were encased by the FGM and FIO, crossing the ischioanal fossa transversely to reach the anal canal, the external anal sphincter, and the skin. This arrangement was bilaterally found in all 24 possible cases. In 17 cases, the connection appeared symmetrical, while in seven cases, it was asymmetrical. The connection mainly consisted of one fiber strand per side, except in one case where there were two fiber strands on one side. The fibers mostly inserted at a sharp angle (23 cases) and in one case at a perpendicular angle.

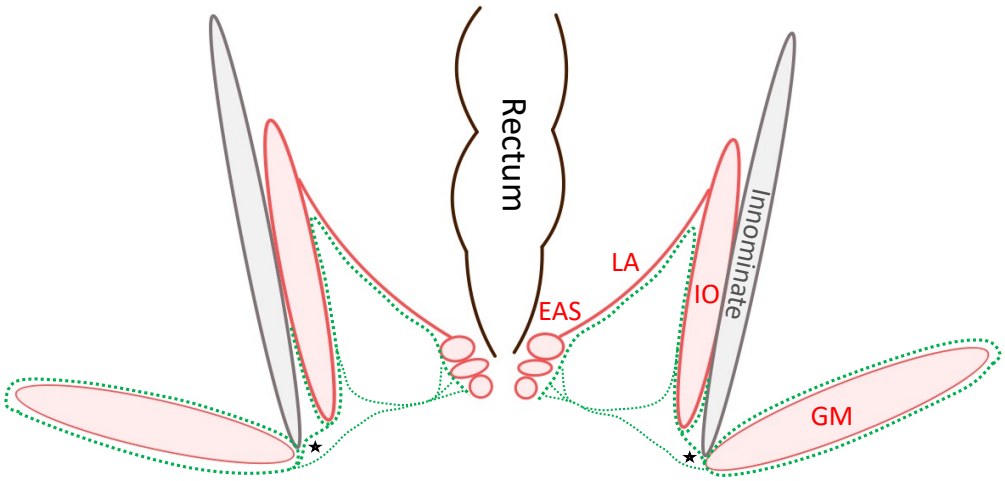

Figure 9: Schematic overview of the fasciae (green dotted lines) in the ischioanal fossa in a coronal section. EAS – External anal sphincter; FGM – Fascia of gluteus maximus; FIO – Fascia of internal obturator; LA – Levator ani (Siess et al., 2023).

In this coronal section, the asterisks indicate the connection between FGM and FIO and, secondly, the relationship of EAS and FGM. The fascial extensions of the gluteus maximus and internal obturator cross the ischioanal fossa transversely while providing a sheathing for the inferior rectal vessels and the inferior rectal nerve.

Connections	***Arrangement***	***Symmetry***	***Fibers per side***	***Insertion angle***
FGM/FIO + EAS	Bilateral	Symmetrical	One per side	Sharp angle
25	24	17	24	23
	Not applicable	Asymmetrical	Multiple per side	Perpendicular
	1	7	1	1
		Not Applicable		Not applicable
		1		1

Table 7: Acquired data on the level of the medial border of the ischial tuberosity/internal obturator in detail.

As this connection consisted of the neurovascular bundles of the inferior rectal vessels and the inferior rectal nerve, all 25 cases morphologically consisted of connective tissue and neurovascular bundles.

Composition		
Connective tissue	Muscle fibers	Neurovascular bundles
25	0	25

Table 8: Composition of the connections at the level of the medial border of the ischial tuberosity/internal obturator.

Deep ischioanal fossa:

The previously described "overlay" of FGM and FIO was connected to the UD in 25 cases, as the branches of the internal pudendal nerve and internal pudendal vessels branched off in this plane. Also, gluteus maximus yielded a direct connection to the urogenital diaphragm alongside the ramus of the ischium and, respectively, the ischial tuberosity. This connection appeared bilateral in all 24 possible cases, with symmetry observed in 18 specimens and asymmetry in six body donors.

Connections	***Arrangement***	***Symmetry***	***Insertion angle***
FGM/FIO + UD	Bilateral	Symmetric	Not applicable
25	24	18	25
	Not applicable	Asymmetric	
	1	6	
		Not Applicable	
		1	

Table 9: Acquired data on the area of the ischioanal fossa in detail.

The connection consisted of connective tissue and neurovascular bundles in all the cases but never contained macroscopically visible muscle fibers.

Composition		
Connective tissue	Muscle fibers	Neurovascular bundles
25	0	25

Table 10: Composition of connections in the area of the ischioanal fossa.

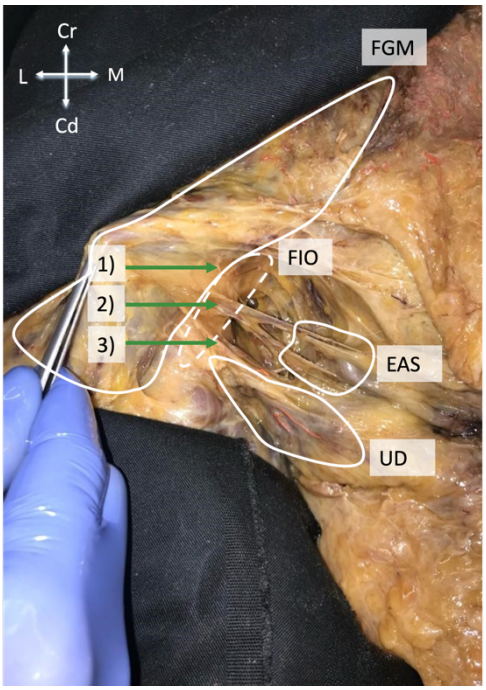

Figure 10: Ischioanal fossa on the left side of a body donor in a supine position. The gluteus maximus is lifted dorsally. EAS – External anal sphincter; FGM – Fascia of gluteus maximus; FIO – Fascia of internal obturator; UD – Urogenital diaphragm (Siess et al., 2023).

In this picture, "1)" represents the connection between the FGM and FIO. The connection between the FGM and EAS, which comprise the inferior rectal vessels and rectal nerve, is indicated as "2)". "3)" marks connective tissue fibers or fascial extensions originating from the FGM and investing into the urogenital diaphragm. This particular connection is utilized for biomechanical testing in the current study.

3.1.3 Sagittal planes

Ischial tuberosity:

In three instances, the connection between the FGM and the FIO was observed. However, in 22 cases, a connection involving the FGM, FIO, and UD was evident. The improvement of preparatory skills throughout the preparation process contributed to a better comprehension and visualization of anatomy and topography. Consequently, the documentation of this connection varied: in the initial three specimens, it was documented as consisting of the FGM and FIO, while in subsequent cases, it was noted as involving the FGM, FIO, and UD.

Connections	*Arrangement*	*Symmetry*
FGM + FIO	Bilateral	Symmetric
3	24	24
FGM + FIO + UD	Not applicable	Not Applicable
22	1	1

Table 11: Acquired data for the ischial tuberosity plane in detail.

In all 25 specimens, the connection was composed of connective tissue.

Composition		
Connective tissue	Muscle fibers	Neurovascular bundles
25	0	0

Table 12: Composition of the connections at the ischial tuberosity plane.

Ischioanal fossa:

Like the findings in the "ischial tuberosity plane," two of the initial three preparations revealed a connection involving just the FGM/FIO and the EAS. In all other cases, there was a connection observed between the FGM/FIO, EAS, and UD. Among the 24 cases, bilateral arrangements were noted, with 17 of them demonstrating symmetry and five displaying asymmetries. In two cases, the connection between the FGM/FIO and EAS was asymmetrical, while the connection between the FGM/FIO and UD was symmetrical.

Connections	*Arrangement*	*Symmetry*
FGM/FIO + EAS	Bilateral	Symmetric
2	24	17
FGM/FIO + EAS + UD	Not applicable	Asymmetric
23	1	5
		Symmetric + asymmetric
		2
		Not Applicable
		1

Table 13: Acquired data of the plane at the ischioanal fossa in detail.

At this level, the inferior rectal vessels and the inferior rectal nerve branched off to the anal canal and the perianal skin. Moving more ventrally, the internal pudendal vessels and the pudendal nerve branched off into their terminal branches to the

UD and perineal region. Consequently, the fiber strands were made up of neurovascular bundles sheathed in connective tissue.

Composition		
Connective tissue	Muscle fibers	Neurovascular bundles
25	0	25

Table 14: Composition of the connections at the plane of the ischioanal fossa.

Pubic symphysis:

At this level, the interpretations of two out of the initial three preparations again differed from those in subsequent dissections. FGM/FIO were found to be connected to the UD twice and to the SAE and UD 23 times. Among these cases, the connections were arranged bilaterally in 24 instances, symmetrically in 17, and asymmetrically in two. Similar to the "ischioanal-fossa-plane," in two cases, the connection between FGM/FIO and EAS was asymmetrical, while the connection between FGM/FIO and UD was found to be symmetrical.

Connections	***Arrangement***	***Symmetry***
FGM/FIO + UD	Bilateral	Symmetrical
2	24	17
FGM/FIO + EAS + UD	Not applicable	Asymmetrical
23	1	2
		Symmetrical + asymmetrical
		2
		Not Applicable
		1

Table 15: Acquired data of the plane at the level of the pubic symphysis in detail.

As above, at this level, the fiber strands were made up of neurovascular bundles sheathed in connective tissue as the inferior rectal vessels and the inferior rectal nerve branched off to the anal canal and the perianal skin. More ventrally, the internal pudendal vessels and the pudendal nerve branched off into their terminal branches to the UD and perineal region.

Composition		
Connective tissue	Muscle fibers	Neurovascular bundles
25	0	25

Table 16: Composition of the connections at the level of the pubic symphysis.

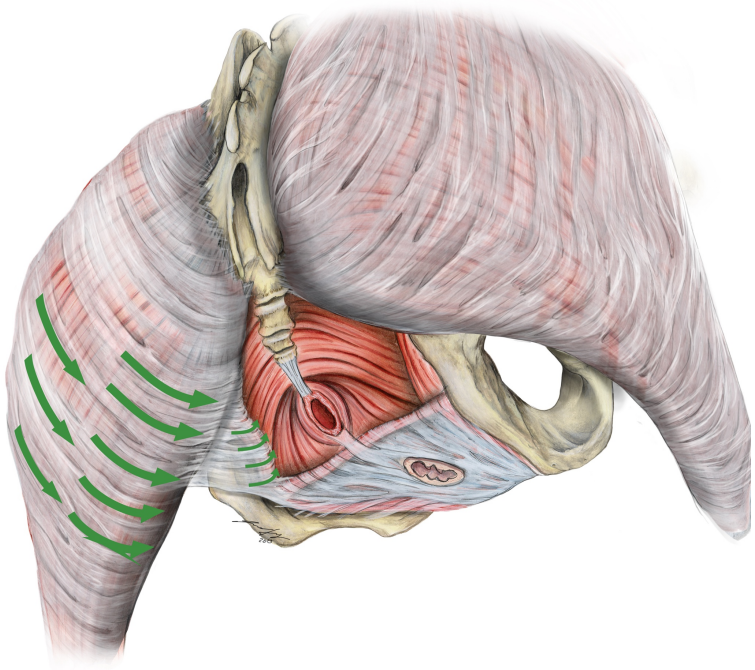

Figure 11: Overview of the topography of the pelvic floor and the gluteus maximus (Siess et al., 2023).

The green arrows mark the pathways of fascial extensions running alongside the gluteus maximus, internal obturator, and urogenital diaphragm.

3.1.4 Plastination

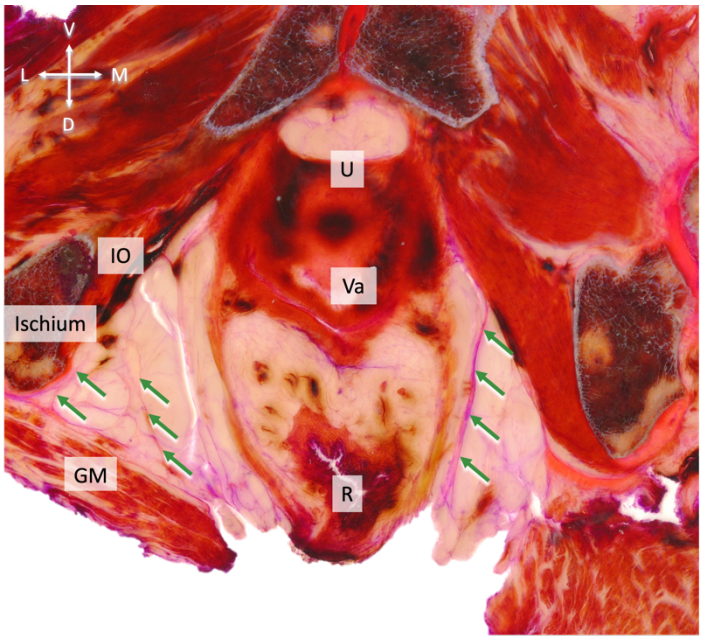

Figure 12: Transverse view of the ischioanal fossa in a thin slice plastinate stained with PAS of an 88-year-old female body. Type III collagen fibers are stained in pink, Type I collagen fibers mostly in dark red. GM – Gluteus maximus; IO – Internal obturator; LA – Levator ani, R – Rectum; U – Urethra; UD – Urogenital diaphragm; V – Vagina (Siess et al., 2023).

The arrows indicate connective tissue fibers within the ischioanal fossa, establishing connections with adjacent muscles including the gluteus maximus, levator ani, internal obturator, and urogenital diaphragm. Notably, the ischioanal fossa lacks muscle fibers. A lamella extends dorsally from the internal obturator, and from this fascia, additional zigzag-aligned fibers extend towards the gluteus maximus.

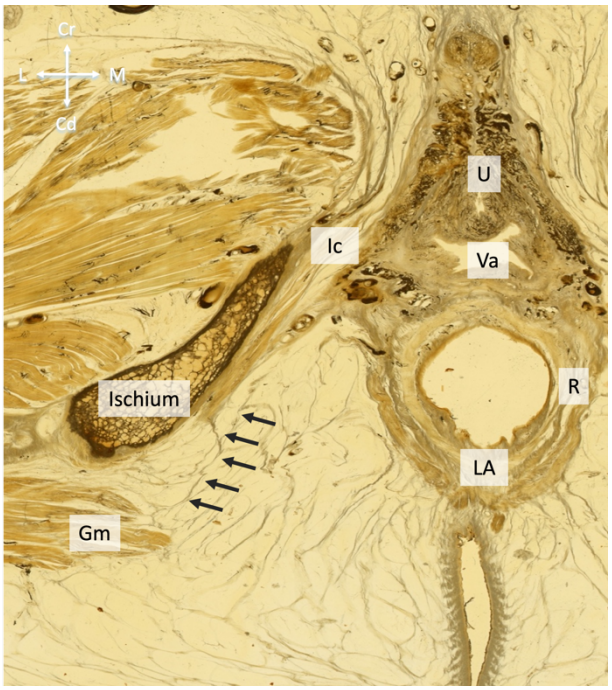

Figure 13: Transverse thin slice plastinate of a 76-year-old female body donor. FGM – fascia of gluteus maximus; LA – Levator ani; Ic – Ischiocavernosus; Is – Ischium; R – rectum; Va – vagina; U – urethra (Siess et al., 2023).

The arrows show connective tissue fibers that originate from the FGM and interconnect with the ischiocavernosus and the urogenital diaphragm, respectively.

3.1.5 Maximum force of the connection between gluteus maximus and the urogenital diaphragm.

In total, 20 samples of ten body donors with an average age of 79 years ±12 years (minimum 57, maximum 94 years) were tested. On average, the maximum force was 23.6 ± 17.8 N with a maximum of 73.4 N and a minimum of 2.6 N.

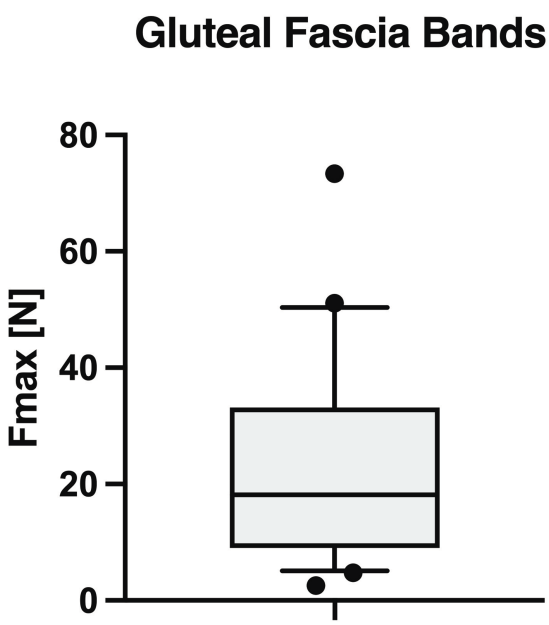

Figure 14: The maximum force (Fmax) the tissues withstood under strain averaged 23.6±17.3 N (range 2.6 to 73.4 N) (Siess et al., 2023).

The detailed results of the biomechanical testing can be found in the attachments.

3.2 Statistical evaluation

In all horizontal planes ($\varphi \geq 0.73$, $p \leq 0.020$), in all sagittal planes ($\varphi = 1.00$, $p \leq 0.040$), and between the horizontal and sagittal ($\varphi \geq 0.77$, $p \leq 0.037$) planes, Cramér φ analyses showed that the connections of the fasciae between gluteus maximus were consistently strong. The detailed statistical data can be found in the attachments.

4 Discussion

The primary goal of the given study was to macroscopically assess the morpho-mechanical connection of the gluteus maximus to the pelvic floor. Secondarily, if such connections could be found, a goal was to investigate their loading capacity on a smaller subset of tissues. Fascial continuations of the gluteus maximus connected it to the internal obturator and the urogenital diaphragm. Covering the borders of the ischioanal fossa, this fascia then extends towards the levator ani. As the inferior rectal nerve and inferior rectal vessels protrude through the pudendal canal, the fasciae of gluteus maximus and internal obturator are also connected to the external anal sphincter, here providing a sheathing for the neurovascular bundles. Macroscopically, throughout the course of the dissections, no muscle fibers were found within this link of connective tissues.

4.1 Dense connections among the gluteus maximus, obturator internus, and the urogenital diaphragm

The dissections illustrated that the sheathing of the inferior rectal vessels and the inferior rectal nerve was not only made up of continuations of the fascia of the internal obturator but also received extensions of the fascia of the gluteus maximus. In their study, Kurihara et al. reported a connection of the pudendal canal to the anal canal and named it the “septum of the ischiorectal space” (Kurihara et al., 2006). This septum divides the ischioanal fossa into two spaces, which they called the “inferior levator space” and “clinical ischiorectal space”. However, the authors did not point out if the septum would originate from just the fascia of the internal obturator or from both, the fasciae of gluteus maximus and obturator internus (Kurihara et al., 2006). One case report described a sigmoid-gluteal abscess with a fistula extending through the ischioanal fossa to the internal obturator (Chadwick et al., 2017), thereby suggesting circumstantial evidence for such a connection. Therefore, it might be asked if this septum and the extension towards the fascia of the gluteus maximus might pose a potential track for fistula formation and, hence, facilitate abscess spread to the gluteal region. Other authors previously described the fascial continuation of gluteus maximus towards the obturator internus fascia: Zhang et al. examined the morphology of the ischioanal fossa in thin slice plastinates of males and reported a “dense strip-fiber connecting with junction fascia

between the obturator internus and gluteus maximus" (Zhang et al., 2017). These strands extend into the fasciae of the internal obturator, gluteus maximus, and levator ani. Up to now, such accurate elucidation for females is missing. De Blok observed "half-circular connective tissue ribbons" which connect the internal obturator, levator ani and gluteus maximus (De Blok, 1982b). Centrally, towards the perineum, the connectives have been portrayed as being sagittal aligned. Laterally, the fibers have been described as having a transverse orientation. The lateral portion had extensions to the fascia of the gluteus maximus, internal obturator and the ischial tuberosity, whereas the medial parts were attached to the superficial perineal fascia. Tunnel-like structures appear to be formed in between these septa (De Blok, 1982a). These findings were approved in the present study. Nevertheless, as the blunt dissection continued into the ventral parts of the ischioanal fossa and adipose tissue was reduced, these "tunnels" were mostly gone. This gives indirect evidence of the function of the collagen connectives in the fossa: the fibers might assist in keeping the adipose tissue in place and to a smaller extent mediate force to the pelvic floor. Even though no macroscopically visible muscle fibers could be found in the ischioanal fossa, a conclusion cannot be drawn with security as Thiel-embalming might have dissolved potential muscle fibers (Zwirner et al., 2019b). Contrary to our findings of the present study, DeBlok found connective tissue fibers, fibroblasts, small blood vessels, and smooth muscle cells in a microscopical analysis of the above-mentioned septa and (De Blok, 1982b). Serial sections of female pelves revealed that the connective tissue builds an entity extending into the different fasciae of the surrounding muscles (De Blok, 1982c). The septa continued medially into the labia majora and superficial perineal fascia (De Blok, 1982c). Laterally, around the ischial tuberosity, a thickening of the covering fascia to an almost skin-like texture was noticed. Steinke describes this as being part of the gluteal suspension system, which has its origin at the ischial tuberosity and extends to the iliotibial tract, the fascia of the gluteus maximus, the aponeuroses of the gluteal muscles ,and the fascia lata (Steinke, 2018). Based on morphological findings, Steinke observed that the gluteal suspension system engages in forming the gluteal sulcus and encloses the inferior border of the gluteus maximus on its way to the ischioanal fossa (Steinke, 2018). The skin-like texture of the gluteal fascia over the ischial tuberosity might be a result of the lateral displacement of the muscle

when bending the hip and sitting down, thereby exposing the fascia underneath (Platzer and Shiozawa, 2018).

In the given experiments Cramer φ analyses and Fisher´s exact test demonstrated a consistency of the fasciae connections and symmetry of gluteus maximus in the aforementioned horizontal and sagittal planes in the female study population. These statistical results indicate that the gluteus maximus contributes consistently to the pelvic floor morpho-mechanics.

4.2 Functional mechanical insights into the connection of gluteus maximus and the urogenital diaphragm

While the given study aimed at investigating the morphological connections between the gluteus maximus and the pelvic floor, Soljanik et al. assessed the role of the ischioanal fossa regarding its functional interaction with the levator ani and gluteus maximus (Soljanik et al., 2012). Using surface electromyography and functional imaging, these researchers studied gluteus maximus and levator ani activity during intentional pelvic floor contraction. Levator ani muscle, gluteus maximus, and the ischioanal fossa showed a synchronous movement in the same direction (Soljanik et al., 2012). Put together, these findings are indicative of the morpho-mechanical interaction of the gluteus maximus and the pelvic floor tissues.

The present study also assessed the load-bearing capacity of the connective tissues within the connection of the fasciae of the gluteus maximus and the urogenital diaphragm. This connection withstood a maximum force similar to connectives in other body regions, such as the dura mater (Zwirner et al., 2019a). This suggests an “in-place-keeping” function and structuring of the adipose tissue for the connective tissues and, to a certain extent, force transmission to the pelvic floor, too. However, as the entity of connective and adipose tissue in the ischioanal fossa forms a three-dimensional network, the overall biomechanical function of this unit cannot entirely be determined, as the given study uniaxially tested fiber strands only located on the lateral border of the ischioanal fossa.

The morpho-mechanical findings presented here offer initial insights into the possible association between the gluteus maximus and the urogenital diaphragm. Excessive tension exerted by the gluteus maximus could theoretically lead to lateral

stress on the sphincters within the pelvic floor, potentially contributing to urinary incontinence. It's worth noting that while the gluteus maximus has been recognized as a muscle that can support urinary continence when appropriately trained, unfavorable loading during single-leg stance could counteract this function, potentially leading to pathological outcomes.

4.3 Limitations

The study population consisted of individuals with an age range of 57 to 86 years. To mitigate the potential bias of aging and menopause and to gain more insights on pelvic floor dysfunction in young female athletes, a younger study cohort would have been more suitable. In future studies, the integration of imaging and functional testing holds the potential to provide valuable insights into the functioning, and potential dysfunction of the pelvic floor in female athletes, as it allows for in-vivo testing. Furthermore, it needs to be noted that the dissection of embalmed tissues poses inherent limitations. Despite careful preparations, the complete structural integrity of the anatomy and topography could not be fully preserved. It is consistent with previous research (Hammer et al., 2015, Zwirner et al., 2019b, Liao et al., 2015, Fessel et al., 2011), that Thiel embalming significantly impacts biomechanical properties to such an extent, rendering it more suitable for preliminary testing (Zwirner et al., 2019b). In comparison to mechanical trials conducted on fresh-frozen tendons, examinations of Thiel-embalmed tendons revealed altered failure characteristics and lower failure stress, indicative of differences in collagen fiber and network composition (Fessel et al., 2011). Consequently, it is essential to acknowledge that the mechanical results obtained in the given study may bear some bias when estimating the true load-bearing capacity of the region. Additionally, it is important to consider that the removal of fat during the Thiel embalming process introduces another methodological limitation (Liao et al., 2015). Given the extensive variability in both the structure and mechanical characteristics of the harvested tissues, the mechanical testing can only be considered preliminary at this stage. If, as suggested by existing literature (Fessel et al., 2011), the specimens used for the mechanical trials indeed possess a softer quality compared to non-embalmed tissue, the connection between the gluteus maximus and the urogenital diaphragm could potentially exhibit a higher load-bearing capacity in fresh specimens.

Consequently, future studies should prioritize the examination of fresh or fresh-frozen tissue samples to obtain more accurate mechanical insights into this connection. Furthermore, it is crucial to standardize the cross-sectional area when testing these tissues, as there is limited prior research addressing maximum force in their testing protocols.

Moreover, it is worth noting that the connective and fatty tissue within the ischioanal fossa form a three-dimensional network. Consequently, uniaxial testing of these samples likely inadequately reflects their in-situ properties to their full extent.

4.4 *Conclusion*

The gluteus maximus exhibits a morphological connection to the pelvic floor through strands of connective tissue investing the nearby muscles. This morpho-mechanical link suggests that, under specific circumstances, the gluteus maximus could potentially play a role in the pathophysiology of urinary stress incontinence. Future research, integrating clinical imaging with in-situ testing like electromyography, may provide further clinical evidence regarding the influence of the gluteus maximus.

5 References

ASHTON-MILLER, J. A., HOWARD, D. & DELANCEY, J. O. 2001. The functional anatomy of the female pelvic floor and stress continence control system. *Scand J Urol Nephrol Suppl*, 1-7; discussion 106-25.

AZPIROZ, F., FERNANDEZ-FRAGA, X., MERLETTI, R. & ENCK, P. 2005. The puborectalis muscle. *Neurogastroenterol Motil,* 17 Suppl 1, 68-72.

BARLEBEN, A. & MILLS, S. 2010. Anorectal anatomy and physiology. *Surg Clin North Am,* 90, 1-15, Table of Contents.

BO, K. 2004. Urinary incontinence, pelvic floor dysfunction, exercise and sport. *Sports Med,* 34, 451-64.

CASEY, E. K. & TEMME, K. 2017. Pelvic floor muscle function and urinary incontinence in the female athlete. *Phys Sportsmed,* 45, 399-407.

CHADWICK, T., KATTI, A. & ARTHUR, J. 2017. Sigmoid-gluteal fistula: a rare complication of fistulating diverticular disease. *J Surg Case Rep,* 2017, rjw237.

DE BLOK, S. 1982a. The connective tissue of the adult female pelvic region. A dissectional analysis. *Acta Morphol Neerl Scand,* 20, 191-212.

DE BLOK, S. 1982b. The connective tissue of the adult female pelvic region. A microscopical analysis. *Acta Morphol Neerl Scand,* 20, 325-46.

DE BLOK, S. 1982c. The connective tissue of the adult female pelvic region. A musculo-fibrous apparatus. *Acta Morphol Neerl Scand,* 20, 347-62.

DELANCEY, J. O. 1994. Structural support of the urethra as it relates to stress urinary incontinence: the hammock hypothesis. *Am J Obstet Gynecol,* 170, 1713-20; discussion 1720-3.

ELIASSON, K., LARSSON, T. & MATTSSON, E. 2002. Prevalence of stress incontinence in nulliparous elite trampolinists. *Scand J Med Sci Sports,* 12, 106-10.

ENCK, P., HINNINGHOFEN, H., MERLETTI, R. & AZPIROZ, F. 2005. The external anal sphincter and the role of surface electromyography. *Neurogastroenterol Motil,* 17 Suppl 1, 60-7.

FESSEL, G., FREY, K., SCHWEIZER, A., CALCAGNI, M., ULLRICH, O. & SNEDEKER, J. G. 2011. Suitability of Thiel embalmed tendons for biomechanical investigation. *Ann Anat,* 193, 237-41.

FRIEDRICH, A., FRANZ, P. & JOHANNES, S. 2012. *Waldeyer - Anatomie des Menschen: Lehrbuch und Atlas in einem Band,* Berlin, Boston, De Gruyter.

FRITSCH, H. & KÜHNEL, W. 2018. *Taschenatlas Anatomie, Band 2: Innere Organe,* Stuttgart Georg Thieme Verlag.

GAN, Z. S. & SMITH, A. L. 2023. Urinary Incontinence in Elite Female Athletes. *Curr Urol Rep,* 24**,** 51-58.

KINTER, K. J. & NEWTON, B. W. 2023. Anatomy, Abdomen and Pelvis, Pudendal Nerve. *StatPearls.* StatPearls [Internet]. Treasure Island (FL): StatPearls Publishing.

KURIHARA, H., KANAI, T., ISHIKAWA, T., OZAWA, K., KANATAKE, Y., KANAI, S. & HASHIGUCHI, Y. 2006. A new concept for the surgical anatomy of posterior deep complex fistulas: the posterior deep space and the septum of the ischiorectal fossa. *Dis Colon Rectum,* 49**,** S37-44.

MARQUES, S. A. A., SILVEIRA, S., PASSARO, A. C., HADDAD, J. M., BARACAT, E. C. & FERREIRA, E. A. G. 2020. Effect of Pelvic Floor and Hip Muscle Strengthening in the Treatment of Stress Urinary Incontinence: A Randomized Clinical Trial. *J Manipulative Physiol Ther,* 43**,** 247-256.

MORGAN, C. N. 1949. The surgical anatomy of the ischiorectal space. *Proc R Soc Med,* 42**,** 189-200.

NAMBIAR, A. K., ARLANDIS, S., BO, K., COBUSSEN-BOEKHORST, H., COSTANTINI, E., DE HEIDE, M., FARAG, F., GROEN, J., KARAVITAKIS, M., LAPITAN, M. C., MANSO, M., ARTEAGA, S. M., RIOGH, A. N. A., O'CONNOR, E., OMAR, M. I., PEYRONNET, B., PHE, V., SAKALIS, V. I., SIHRA, N., TZELVES, L., VAN POELGEEST-POMFRET, M. L., VAN DEN BOS, T. W. L., VAN DER VAART, H. & HARDING, C. K. 2022. European Association of Urology Guidelines on the Diagnosis and Management of Female Non-neurogenic Lower Urinary Tract Symptoms. Part 1: Diagnostics, Overactive Bladder, Stress Urinary Incontinence, and Mixed Urinary Incontinence. *Eur Urol,* 82**,** 49-59.

NYGAARD, I. E. & HEIT, M. 2004. Stress urinary incontinence. *Obstet Gynecol,* 104**,** 607-20.

PETROS, P. E. & ULMSTEN, U. I. 1990. An integral theory of female urinary incontinence. Experimental and clinical considerations. *Acta Obstet Gynecol Scand Suppl,* 153**,** 7-31.

PIRES, T., PIRES, P., MOREIRA, H. & VIANA, R. 2020. Prevalence of Urinary Incontinence in High-Impact Sport Athletes: A Systematic Review and Meta-Analysis. *J Hum Kinet,* 73**,** 279-288.

PLATZER, W. & SHIOZAWA, T. 2018. Dorsale Hüftmuskeln, Fortsetzung. *In:* PLATZER, W. & SHIOZAWA, T. (eds.) *Taschenatlas Anatomie, Band 1: Bewegungsapparat.* 12., aktualisierte Auflage ed.: Georg Thieme Verlag KG.

ROBERTS, W. H., HABENICHT, J. & KRISHINGNER, G. 1964. The Pelvic and Perineal Fasciae and Their Neural and Vascular Relationships. *Anat Rec,* 149**,** 707-20.

SAM, P., NASSEREDDIN, A. & LAGRANGE, C. A. 2023. Anatomy, Abdomen and Pelvis: Bladder Detrusor Muscle. *StatPearls.* Treasure Island (FL).

SCHOLZE, M., SAFAVI, S., LI, K. C., ONDRUSCHKA, B., WERNER, M., ZWIRNER, J. & HAMMER, N. 2020. Standardized tensile testing of soft tissue using a 3D printed clamping system. *HardwareX,* 8**,** e00159.

SCHÜNKE, M.-. 2022a. *Prometheus LernAtlas der Anatomie Allgemeine Anatomie und Bewegungssystem,* Stuttgart New York, NY, Georg Thieme Verlag.

SCHÜNKE, M.-. 2022b. *Prometheus LernAtlas der Anatomie Innere Organe,* Stuttgart New York, Georg Thieme Verlag.

SIESS, M., STEINKE, H., ZWIRNER, J. & HAMMER, N. 2023. On the potential morpho-mechanical link between the gluteus maximus muscle and pelvic floor tissues (manuscript submitted for publication). Scientific Reports

SOLJANIK, I., JANSSEN, U., MAY, F., FRITSCH, H., STIEF, C. G., WEISSENBACHER, E. R., FRIESE, K. & LIENEMANN, A. 2012. Functional interactions between the fossa ischioanalis, levator ani and gluteus maximus muscles of the female pelvic floor: a prospective study in nulliparous women. *Arch Gynecol Obstet,* 286**,** 931-8.

SORA, M. C., LATORRE, R., BAPTISTA, C. & LOPEZ-ALBORS, O. 2019. Plastination-A scientific method for teaching and research. *Anat Histol Embryol,* 48**,** 526-531.

STEINKE, H. 2018. *Atlas of human fascial topography,* Leipzig, Leipziger Universitätsverlag.

STEINKE, H., WIERSBICKI, D., SPECKERT, M. L., MERKWITZ, C., WOLFSKAMPF, T. & WOLF, B. 2018. Periodic acid-Schiff (PAS) reaction and plastination in whole body slices. A novel technique to identify fascial tissue structures. *Ann Anat,* 216**,** 29-35.

STROHBEHN, K. 1998. Normal pelvic floor anatomy. *Obstet Gynecol Clin North Am,* 25**,** 683-705.

THIEL, W. 1992a. [An arterial substance for subsequent injection during the preservation of the whole corpse]. *Ann Anat,* 174**,** 197-200.

THIEL, W. 1992b. [The preservation of the whole corpse with natural color]. *Ann Anat,* 174**,** 185-95.

THIEL, W. 2002. [Supplement to the conservation of an entire cadaver according to W. Thiel]. *Ann Anat,* 184**,** 267-9.

VLEEMING, A., SCHUENKE, M. D., MASI, A. T., CARREIRO, J. E., DANNEELS, L. & WILLARD, F. H. 2012. The sacroiliac joint: an overview of its anatomy, function and potential clinical implications. *J Anat,* 221**,** 537-67.

VON HAGENS, G. 1985. *Heidelberger Plastinationshefter. Heidelberg Plastination Folder. Sammlung aller Merkblätter zur Plastination. ,* Heidelberg, Eigenverlag Anatomisches Institut I/Biodur Heidelberg.

WALLNER, C., DABHOIWALA, N. F., DERUITER, M. C. & LAMERS, W. H. 2009. The anatomical components of urinary continence. *Eur Urol,* 55**,** 932-43.

WANG, Y. H. W. & WISEMAN, J. 2023. Anatomy, Abdomen and Pelvis, Rectum. *StatPearls.* Treasure Island (FL).

WILKE, H. J., WERNER, K., HAUSSLER, K., REINEHR, M. & BOCKERS, T. M. 2011. Thiel-fixation preserves the non-linear load-deformation characteristic of spinal motion segments, but increases their flexibility. *J Mech Behav Biomed Mater,* 4**,** 2133-7.

WILLIAMS, A. M. M., SATO-KLEMM, M., DEEGAN, E. G., EGINYAN, G. & LAM, T. 2022. Characterizing Pelvic Floor Muscle Activity During Walking and

Jogging in Continent Adults: A Cross-Sectional Study. *Front Hum Neurosci,* 16**,** 912839.

WONG, M., SINKLER, M. A. & KIEL, J. 2022. Anatomy, Abdomen and Pelvis, Sacroiliac Joint. *StatPearls.* Treasure Island (FL).

ZAUNBRECHER, N., ARBOR, T. C. & SAMRA, N. S. 2023. Anatomy, Abdomen and Pelvis: Internal Iliac Arteries. *StatPearls.* Treasure Island (FL) ineligible companies.

ZHANG, J. F., DU, M. L., SUI, H. J., YANG, Y., ZHOU, H. Y., MENG, C., QU, M. J., ZHANG, Q., DU, B. & FU, Y. S. 2017. Investigation of the ischioanal fossa: Application to abscess spread. *Clin Anat,* 30**,** 1029-1033.

ZWIRNER, J., ONDRUSCHKA, B., SCHOLZE, M., SCHULZE-TANZIL, G. & HAMMER, N. 2019a. Mechanical and morphological description of human acellular dura mater as a scaffold for surgical reconstruction. *J Mech Behav Biomed Mater,* 96**,** 38-44.

ZWIRNER, J., SCHOLZE, M., ONDRUSCHKA, B. & HAMMER, N. 2019b. Tissue biomechanics of the human head are altered by Thiel embalming, restricting its use for biomechanical validation. *Clin Anat,* 32**,** 903-913.

6 Attachment

Statistical evaluation

Symmetry

	Level 2 horizontal	Cramér φ	Level 3 horizontal	Cramér φ	Level 1 sagittal	Cramér φ	Level 2 sagittal	Cramér φ	Level 3 sagittal	Cramér φ
Level 1 horizontal	p=0.020	.741	p=0.013	.752	p=0.040	1	p=0.037	.770	p=0.037	.770
Level 2 horizontal			p=0.028	.731	p=0.040	1	<.001	.908	<.001	.908
Level 3 horizontal					p=0.040	1	<.001	.846	<.001	.846
Level 1 sagittal							p=0.040	1	p=0.040	1
Level 2 sagittal									<.001	1

Figure 15: Fisher´s exact test and Cramer φ analysis of symmetry.

Connections

	Level 2 horizontal	Cramér φ	Level 3 horizontal	Cramér φ	Level 1 sagittal	Cramér φ	Level 2 sagittal	Cramér φ	Level 3 sagittal	Cramér φ
Level 1 horizontal	Const	-	Const	-	Const	1	Const	-	Const	-
Level 2 horizontal			Const	-	Const	1	Const	-	Const	-
Level 3 horizontal					Const	1	Const	-	Const	-
Level 1 sagittal							p=0.010	.799	p=0.010	.799
Level 2 sagittal									p=0.003	1

Figure 16: Fisher´s exact test and Cramer φ analysis of the connections.

Biomechanical testing

Sample No.	F_{max} in N
J152	24.5
J152.2	31.24
J147	73.37
J147.2	8.4
J88	37.75
J88.2	13.05
J70	17.92
J70.2	30.77
J49	8.58
J49.2	10.08
J141	33.82
J141.2	51.11
J55	43.64
J55.2	17.13
J160	13.74
J160.2	23.03
J126	18.4
J126.2	8.32
J50	2.58
J50.2	4.75

Table 17: Biomechanical results in detail.

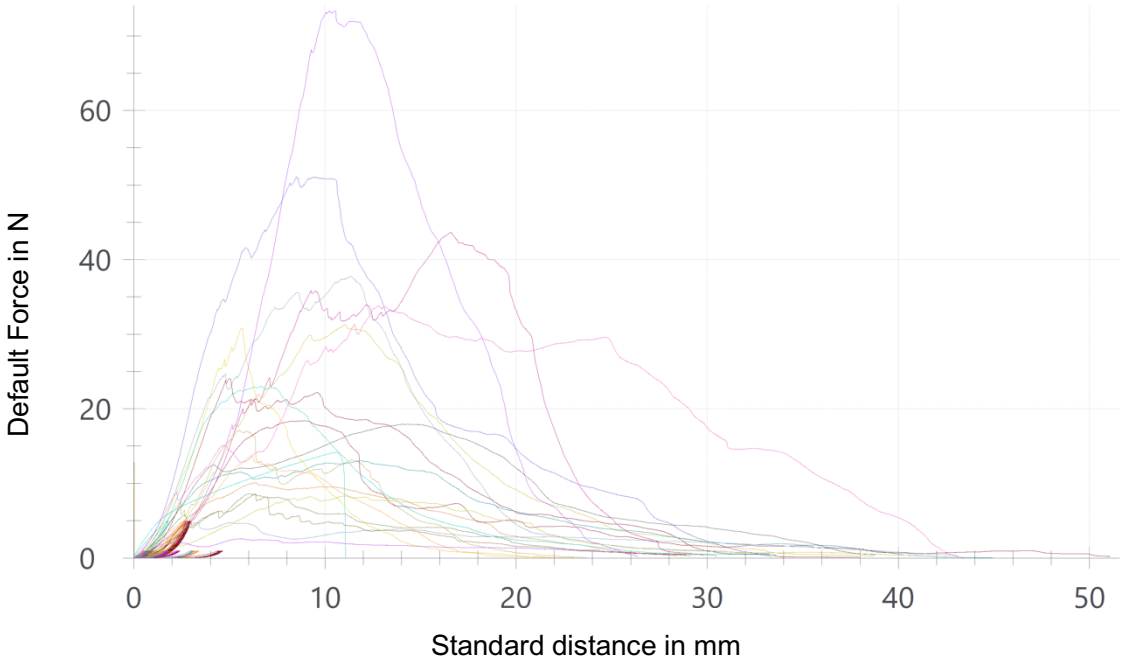

Figure 17: Graphical display of the biomechanical test results.

The case report form

Case Report Form

General
No.: Sex: Relevant pre-existing conditions:

Macroscopic assessment after dissection: (specimen in a prone position)

Horizontal planes
1st plane: skin level plane

Arrangement:
☐ Unilateral
☐ Bilateral

☐ Symmetrical
☐ Asymmetrical

Quantity of fibres: ____

Insertion:
☐ perpendicular
☐ sharp angle
☐ flat angle

Connections consist of…:
☐ connective tissue
☐ muscle fibres
☐ neurovascular bundles

Connections between _____and_____.
Notes:

2nd plane: pudendal canal/upper border of the internal obturator/falciform process

Arrangement:
☐ Unilateral
☐ Bilateral

☐ Symmetrical
☐ Asymmetrical

Quantity of fibres: ____

Insertion:
☐ perpendicular
☐ sharp angle
☐ flat angle

Connections consist of…:
☐ connective tissue
☐ muscle fibres
☐ neurovascular bundles

Connections between _____and_____.
Notes:

Pictures: No. Version 8.0 1

3rd plane: deep ischioanal fossa/cranial to the pudendal canal

Arrangement:
☐ Unilateral
☐ Bilateral

☐ Symmetrical
☐ Asymmetrical

Quantity of fibres: ____

Insertion:
☐ perpendicular
☐ sharp angle
☐ flat angle

Connections consist of…:
☐ connective tissue
☐ muscle fibres
☐ neurovascular bundles

Connections between _____and_____:
Notes:

Pictures: No. Version 8.0 2

Sagittal planes

1st plane: medial border of the ischial tuberosity/internal obturator muscle

Arrangement:
☐ Unilateral
☐ Bilateral

☐ Symmetrical
☐ Asymmetrical

Connections consist of…:
☐ connective tissue
☐ muscle fibres
☐ neurovascular bundles

Connections between _____and_____.
Notes:

2nd "area": ischioanal fossa

Arrangement:
☐ Unilateral
☐ Bilateral

☐ Symmetrical
☐ Asymmetrical

Connections consist of…:
☐ connective tissue
☐ muscle fibres
☐ neurovascular bundles

Connections between _____and_____.
Notes:

3rd plane: pubic symphysis/pelvic diaphragm/urogenital diaphragm

Arrangement:
☐ Unilateral
☐ Bilateral

☐ Symmetrical
☐ Asymmetrical

Connections consist of…:
☐ connective tissue
☐ muscle fibres
☐ neurovascular bundles

Connections between _____and_____.
Notes:

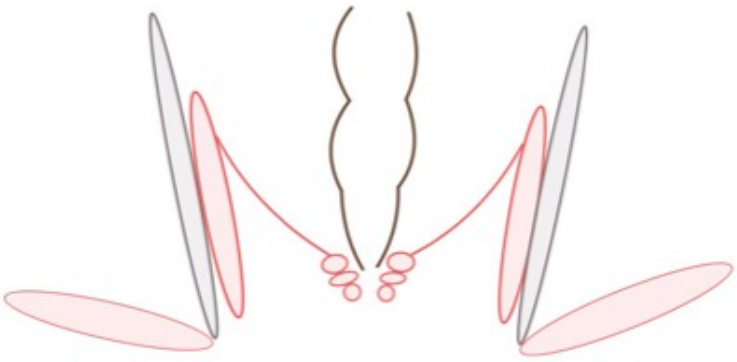

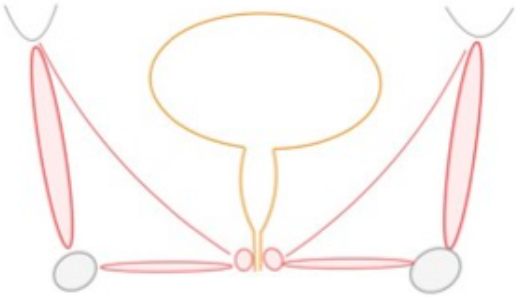

Pictures: No. Version 8.0 4